

Near-Complete Correction of Profound Metabolomic Impairments Corresponding to Functional Benefit in MPS IIIB Mice after IV rAAV9-hNAGLU Gene Delivery

Haiyan Fu,^{1,2} Aaron S. Meadows,¹ Tierra Ware,¹ Robert P. Mohny,³ and Douglas M. McCarty^{1,2}

¹Center for Gene Therapy, The Research Institute at Nationwide Children's Hospital (NCH-RI), Columbus, OH 43205, USA; ²Department of Pediatrics, College of Medicine and Public Health, The Ohio State University, Columbus, OH 43202, USA; ³Metabolon, Inc., Durham, NC 27713, USA

Mucopolysaccharidosis (MPS) IIIB is a lysosomal storage disease with complex CNS and somatic pathology due to a deficiency in α -N-acetylglucosaminidase (NAGLU). Using global metabolic profiling by mass spectrometry targeting 361 metabolites, this study detected significant decreases in 225 and increases in six metabolites in serum samples from 7-month-old MPS IIIB mice, compared to wild-type (WT) mice. The metabolic disturbances involve virtually all major pathways of amino acid, peptide (58/102), carbohydrate (18/28), lipid (111/139), nucleotide (12/24), energy (2/9), vitamin and cofactor (11/16), and xenobiotic (11/28) metabolism. Notably, the reduced metabolites included eight essential amino acids, vitamins (C, E, B2, and B6), and neurotransmitters (serotonin, glutamate, aspartate, tryptophan, and N-acetyltyrosine). The metabolic impairments appear to emerge early during disease progression before the age of 2 months. Importantly, the restoration of NAGLU activity with an intravenous (i.v.) injection of rAAV9-hNAGLU vector led to near-complete correction of all serum metabolite abnormalities, with 201 (87%) metabolites normalized and 30 (13%) over-corrected. While the mechanisms are unclear, our data demonstrate that the lack of NAGLU activity triggers profound functional metabolic disturbances in MPS IIIB. These metabolic impairments respond well to a systemic rAAV9-hNAGLU gene delivery, supporting the surrogate biomarker potential of serum metabolomic profiles for MPS IIIB therapies.

INTRODUCTION

Mucopolysaccharidosis (MPS) IIIB (Online Mendelian Inheritance in Man [OMIM]: 252920) is an autosomal recessive disorder caused by mutations in the gene that encodes α -N-acetylglucosaminidase (NAGLU), a lysosomal acid hydrolase that is essential in the stepwise degradation of heparan sulfate (HS) glycosaminoglycans (GAG).¹ The resulting enzyme deficiency leads to a buildup of HS-GAGs within the lysosomes. The disease-causing alleles of MPS IIIB are highly polymorphic, with over 80 mutations identified.² The lysosomal accumulation of HS-GAGs results in clinical disease, presenting predominantly severe progressive neurological disorders. Somatic manifestations of MPS IIIB do occur in all patients, but are mild, relative to other forms of MPS. Infants appear normal at birth but develop

profound neurological manifestation at the age of 3–4 years, including reduced cognitive capacity, hyperactivity, seizures, and ultimately death.²

The primary pathology of MPS IIIB has been characterized as the accumulation of HS-GAGs in lysosomes in cells of virtually all tissues/organs, especially in the CNS involving both neuronal and non-neuronal cells.^{1,3} While detailed mechanisms of pathology, especially the neuropathology of MPS III, are not yet well understood, numerous studies have reported cascades of complex secondary pathological events in the CNS, including broad metabolic impairments,^{4–6} neuroinflammation,^{5,7–11} oxidative stress,^{10,12} autophagy,^{13,14} and neurodegeneration.^{7,9,11,15–20} It is worth noting that many of these secondary neuropathological features of MPS IIIB, such as β -amyloid (A β) aggregation,^{15,18} tauopathy,^{17,18} synucleinopathy,^{16,19} oxidative stress,^{10,12} and neuroinflammation,^{5,7–11} are also common hallmarks of other neurodegenerative diseases like Alzheimer's (AD)^{21,22} and Parkinson's disease (PD).^{23,24} In addition, our recent studies demonstrate widespread profound neuropathology in the peripheral nervous system (PNS),²⁵ indicating that neuropathological manifestation affects the entire nervous system.

No definite treatment is currently available for MPS IIIB and therapies have been limited to palliative treatment. The greatest challenge in developing therapies for MPS III has been the presence of the blood-brain barrier (BBB). Significant therapeutic advancements have been made for treating lysosomal storage diseases (LSDs), such as hematopoietic stem cell transplantation (HSCT), recombinant enzyme replacement therapy (ERT), and gene therapy.²⁶ MPS III (A–D) disorders are not amenable to currently approved systemic ERT or HSCT, which have shown somatic benefits, since the BBB precludes effective CNS access to either recombinant enzyme or enzyme produced by transplanted hematopoietic stem cells. Alternative intrathecal ERT clinical trials are ongoing, targeting the CNS disorders in

Received 10 October 2016; accepted 25 December 2016;
<http://dx.doi.org/10.1016/j.ymthe.2016.12.025>.

Correspondence: Haiyan Fu, Center for Gene Therapy, The Research Institute at Nationwide Children's Hospital, Columbus, OH 43205, USA.

E-mail: haiyan.fu@nationwidechildrens.org

patients with MPS I, II, and IIIA, and they require repetitive administration on a regular basis. Gene therapy has been considered an ideal approach for treating LSDs, because of the potential for long-term endogenous production of recombinant enzymes without the need to treat every cell. Numerous virus-mediated gene therapy studies, mostly designed to restore the missing enzyme activity, have shown varying degrees of correction of lysosomal storage in vitro and in vivo in LSD animal models, using various viral vectors.²⁷ Recombinant adeno-associated virus (rAAV) has been a favored vector for gene delivery because it is non-pathogenic, with demonstrated long-term expression in the CNS and periphery.^{27,28} The recent finding of trans-BBB neurotropism of AAV9 offers an effective solution for CNS gene therapy, showing great potential for the treatment of LSDs and other neurological diseases.^{29–33} A single systemic delivery of rAAV9 vectors can lead to global CNS and widespread somatic restoration of enzyme activity, correction of lysosomal storage pathology, and functional neurological benefits in mice with MPS IIIB or IIIA.^{29,30}

As therapeutic development advances and more therapies for MPS become available, the lack of accessible biomarkers will be a critical challenge for therapeutic assessment. Urinary GAGs and specific lysosomal enzymes have been the only biomarkers for MPS, although recent studies identified serum heparin cofactor II-thrombin (HCII-T) as a biomarker for MPS I, II, and III;³⁴ dipeptidyl peptidase IV (DPP-IV) for MPS I, II, III, IVA, and VI;³⁵ and recently the potential of disease-specific non-reducing end carbohydrate biomarkers for MPS.³⁶ However, there are currently no specific biomarkers for MPS corresponding to neurological disease severity or therapeutic responsiveness. The critical challenge for finding CNS-specific biomarkers stems from limited access to the CNS tissues of patients, especially at early disease stages.

In this study, a global metabolomic profiling approach using mass spectrometry (MS) was performed to identify metabolomic impairments in MPS IIIB mice and assess their responses to our established systemic rAAV9-hNAGLU gene delivery approach.

RESULTS

In this study, we performed global metabolomic analyses on serum samples from MPS IIIB mice and their wild-type (WT) littermates, at ages 2 and 7 months, to investigate metabolomic abnormalities during the disease progression in MPS IIIB. To assess the biomarker potential of serum metabolic profiling for MPS IIIB, we treated a cohort of MPS IIIB mice with an intravenous (i.v.) injection of 5×10^{12} vg/kg rAAV9-CMV-hNAGLU at age 1 month ($n = 19$, male-to-female ratio [M:F] = 10:9). Non-treated MPS IIIB ($n = 15$, M:F = 8:7) and WT ($n = 16$, M:F = 8:8) littermates were used for metabolic studies and as controls. All non-treated MPS IIIB ($n = 15$) and WT ($n = 16$) mice and 13 AAV-treated MPS IIIB mice were tested for behavior performance in a hidden task in the Morris water maze at age 5–5.5 months. Necropsies were performed at ages 2 and 7 months ($n = 6$ /group, M:F = 1:1). Tissues were assayed for rNAGLU activity and GAG contents ($n = 6$ /group). Serum samples were assayed for

global metabolomic profiles ($n = 6$ /group). Animals also were observed for longevity ($n > 7$ /group). Serotype 9 rAAV vectors cross the BBB, and a systemic rAAV9-CMV-hNAGLU delivery previously was shown to result in both CNS and somatic correction of pathology in MPS IIIB mice.^{29,37}

Mass Spectrometry Provides Decisive MPS IIIB Metabolomic Profiles

Global metabolomic profiling by mass spectrometry was performed on the serum samples from MPS IIIB and WT mice at ages 2 and 7 months to assess metabolic abnormalities during the disease progression. Principal-component analyses (PCAs) (Figure 1A) and heatmap analyses (Figure 1B) of the 361 metabolites showed clear separation of serum metabolomic profiles in 7-month-old MPS IIIB mice from those of age-matched WT mice and the rest of the experimental groups, with the exception of one WT mouse that appeared to be an outlier. This WT outlier could not be re-genotyped due to tissue availability, and it was maintained in all data analyses, which would increase the biological variation of the WT group and likely reduce the number of significant differences in comparison to this group (Table S1). Even so, this clear division indicates that the detected metabolomic abnormalities are highly likely to be MPS IIIB associated and that global metabolomic profiling may have potential for the identification of pathological metabolomic signatures during MPS IIIB disease progression.

Global Metabolomics Revealed Broad Profound Metabolism Impairments during Disease Progression in MPS IIIB Mice

Using MS, we detected significant changes ($p \leq 0.05$) in 18 metabolites (8%) at the age of 2 months and 231 metabolites (64%) at the age of 7 months in MPS IIIB mice (Table 1), in comparison to their WT littermate controls. The majority of the altered serum metabolites were significantly reduced in MPS IIIB mice compared to WT, with 17 (94.4%) decreased and one (5.6%) increased at the age of 2 months and 225 (97.4%) decreased and six (2.6%) increased at the age of 7 months (Table 1). Furthermore, the detected metabolomic impairments in MPS IIIB mice were associated with broad, virtually all, metabolic pathways, involving the metabolism of amino acids (58/102), carbohydrates (18/28), lipids (111/139), peptides (8/15), nucleotides (12/24), energy (2/9), vitamin and cofactors (11/16), and xenobiotics (11/28) (Table 2; Table S1). These data indicate that MPS IIIB triggers profound metabolic suppression that may emerge early during the disease progression. Data presented below are mainly focused on serum metabolite changes in MPS IIIB mice at the age of 7 months.

Notably, in 7-month-old MPS IIIB mice, the reduced serum metabolites included eight essential (8/9), five conditionally essential (5/7), and four non-essential (4/4) amino acids (Figure 2), indicating broad functional defects from absorption to biosynthesis of amino acids. Our results also showed a significant disturbance in branched-chain amino acid pathways (Figure S2) and urea cycle (Figure S3). Importantly, we also detected significant reductions in serum amino acids and derivatives that can function as key neurotransmitters or components critical in neurotransmitter metabolism, including serotonin, tryptophan, 5-hydroxyindoleacetate, dihydrobiopterin, glutamate,

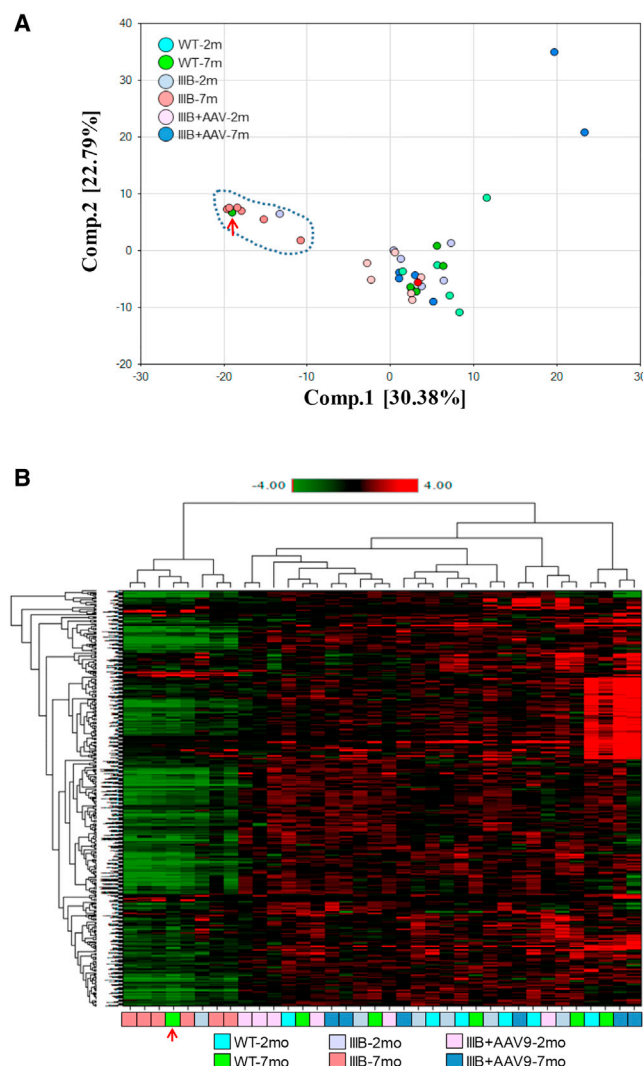


Figure 1. Profound Metabolic Impairments in MPS IIIB Mice and Metabolic Responses to a Systemic rAAV9-CMV-hNAGLU Gene Delivery
 Mouse serum samples were analyzed by global metabolomic profiling using mass spectrometry at the age of 2 or 7 months ($n = 6/\text{group}$). (A) Principal-component analyses and (B) heatmap analysis are shown. WT, wild-type mice; IIIB, MPS IIIB mice; IIIB + AAV, MPS IIIB mice treated at age 1 month with an i.v. injection of 5×10^{12} vg/kg rAAV9-CMV-hNAGLU; red arrows, outlier.

4-hydroxybutyric acid, proline, N-acetyltyrosine, and phenylalanine (Figure 3). Significant decreases also were observed in multiple serum metabolites that are considered to be critical in neurological functions, such as acetylcarnitine (ALC), N-acetylaspartate (NAA), kynurenine, and scyllo-inositol (Table S1).

Of reduced serum carbohydrate metabolites in MPS IIIB mice, there were known essential components of protein and lipid glycosylation pathways, such as glucose, fructose, erythronate, mannose, N-acetylglucosamine, N-acetylneuraminic acid, and fucose (Figure 4; Table 2; Table S1). Our data also showed an extensive disturbance in lipid

Table 1. Profound Metabolic Abnormalities in MPS IIIB Mice

Groups	Age (Months)	Number of Metabolites ($p \leq 0.05$)		
		Decrease	Increase	Total
IIIB/WT	2	17	1	18
IIIB/WT	7	225	6	231

Serum samples were assayed for 361 metabolites at 2 and 7 months of age, using mass spectrometry. IIIB, MPS IIIB mice; WT, wild-type littermates of MPS IIIB mice.

metabolism in MPS IIIB mice, with a significant alteration in the majority of measured lipid metabolites (111/139, 80%), all down, involving virtually all lipid classes measured, including fatty acids, lipids, sterols, steroid (corticosterone), and others (Table 2; Table S1). Furthermore, we observed a significant decrease in serum metabolites that are critical for the metabolism pathways of vitamins and cofactors (11/16), including vitamin C (ascorbate, gulono-1,4-lactone, threonate, arabinonate, and oxalate), E (alpha-tocopherol), B6 (pyridoxate), B5 (pantothenate), B2 (flavin adenine dinucleotide), B3 (nicotinamide), and dihydrobiopterin (Figure S3; Table 2; Table S1). It is, therefore, not surprising to see the reduction of metabolites indicating lowered energy production (Figure S4).

Therapeutic Gene Delivery to Assess the Biomarker Potential of Serum Metabolomic Profiles for MPS IIIB

To determine the CNS therapeutic surrogate potential of serum metabolomic profiles for MPS IIIB, we treated 1-month-old MPS IIIB mice ($n = 15$) with a single intravenous injection of rAAV9-CMV-hNAGLU vector (5×10^{12} vg/kg). Tissue analyses, behavior testing, and longevity observation were performed to assess the therapeutic impacts of the rAAV9 gene delivery.

Widespread CNS and Somatic Restoration of NAGLU Activity and Functional Benefits of Systemic rAAV-hNAGLU Gene Delivery in MPS IIIB Mice

At the ages of 2 and 7 months ($n = 6/\text{group}$), tissues were assayed for NAGLU enzymatic activity to assess the expression and functionality of the transgene. We detected NAGLU activity at normal or sub-normal levels in the brain, spleen, and lung; supra-physiologic levels in the liver, skeletal muscles, and heart; and low levels in the intestine and kidney (Figure 5A). No detectable NAGLU activity (<0.03 unit/mg) was observed in tissues from non-treated MPS IIIB mice.

Tissues also were assayed for GAG content to quantify the impact of rAAV9-NAGLU gene delivery on the lysosomal storage pathology in MPS IIIB mice. The treatment resulted in a reduction of GAG content to normal levels in the brain, liver, heart, lung, intestine, spleen, and skeletal muscle, but with only a partial reduction of GAG in the kidney (Figure 5B). These data indicate that rAAV9-mediated hNAGLU is functional and sufficient for the correction of lysosomal storage pathology in both the CNS and somatic tissues.

The animals were tested for behavior in a hidden task in the Morris water maze when they were 5–5.5 months old ($n = 13$, M:F = 7:6).

Table 2. Broad Metabolism Pathway Impairments in MPS IIIB Mice

Pathways	No. of Metabolites Assayed	Number of Metabolites Changed ($p \leq 0.05$) ^a	
		Age 2 Months	Age 7 Months
Amino acids	102	6	58
Carbohydrates	28	0	18
Lipids	139	9	111
Peptides	15	1	8
Nucleotides	24	0	12
Energy	9	0	2
Cofactors and vitamins	16	0	11
Xenobiotics	28	2	11
Total	361	18	231

Serum samples were assayed for 361 metabolites at 2 and 7 months of age using mass spectrometry.

^aChanges in MPS IIIB mice versus WT.

Similar to our previously published data,^{29,37} rAAV9-treated MPS IIIB mice exhibited significant improvement in latency to find a hidden platform and swimming ability in the water maze (Figure 5C), indicating the functional correction of neurological disorders. Seven rAAV9-treated animals were observed for longevity, showing significantly improved survival with a lifespan of 6–24 months, of which the majority lived within the lifespan of WT mice (Figure 5D, $p > 0.05$). In contrast, non-treated MPS IIIB mice died at 7.2–13.5 months of age (Figure 5D) ($p < 0.0001$ versus WT or AAV-treated MPS IIIB mice). These data further support the functional neurological benefits of the rAAV9 gene delivery, since premature death in MPS IIIB has been attributed to neurological disorders.

Rapid and Persistent Correction of the Profound Metabolic Impairments

At the ages of 2 and 7 months ($n = 6$ /group), serum samples from rAAV9-hNAGLU-treated MPS IIIB mice were analyzed by global metabolomic profiling using mass spectrometry, to assess the responsiveness and surrogate biomarker potential of serum metabolomic profiles for MPS IIIB. Data from non-treated MPS IIIB and WT littermates were used as controls.

Our results showed the correction of all 231 significantly altered serum metabolites in the rAAV9-hNAGLU-treated MPS IIIB mice, when tested at the age of 7 months (Table 3; Figure 1; Table S1), of which 201 (87%) were normalized. Notably, over-corrections were observed in 30 (13%) of 225 significantly decreased metabolites and in 27 metabolites that were decreased, but not statistically significant ($p > 0.05$), in non-treated MPS IIIB mice at the age of 7 months (Table S1). Similarly, at the age of 2 months (1 month post-injection [pi]), our data showed the correction of 89% (16/18) of the significantly altered metabolites in rAAV9-treated MPS IIIB mice, with eight metabolites significantly decreased, including two that were not corrected (Table 3; Figure 1; Table S1). Importantly, following a single i.v. rAAV9-hNAGLU gene delivery, the rapid and persistent func-

tional correction of the profound metabolomic impairments (Table 3; Table S1; Figures 2 and 4; Figures S1–S4) correlated with the effective restoration of NAGLU activity, clearance of GAG storage, normalization of behavior performance, and extended survival in MPS IIIB mice (Figure 5).

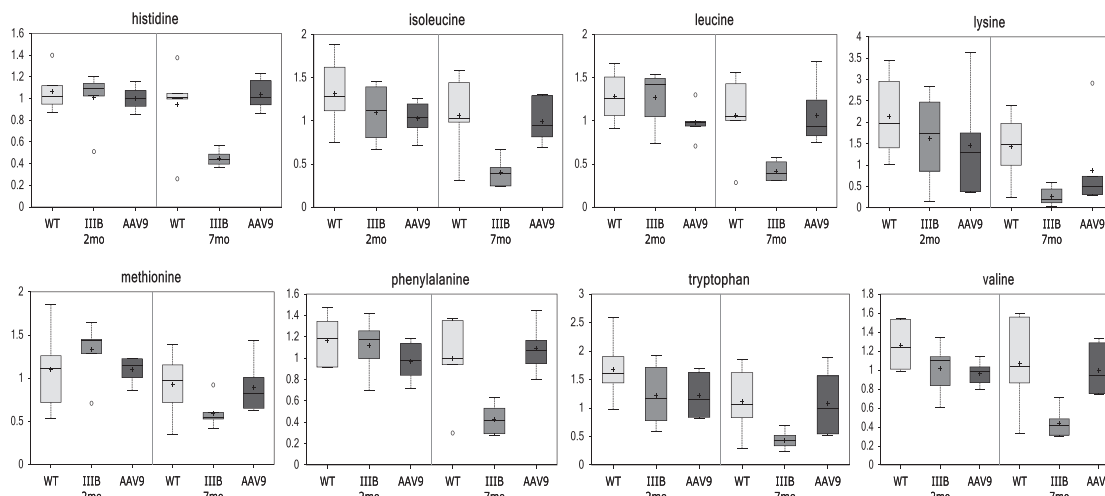
DISCUSSION

We demonstrate here that MPS IIIB triggers profound metabolic impairments, and serum global metabolomic profiles may offer great potential as biomarkers for MPS IIIB disease progression and therapeutic assessments.

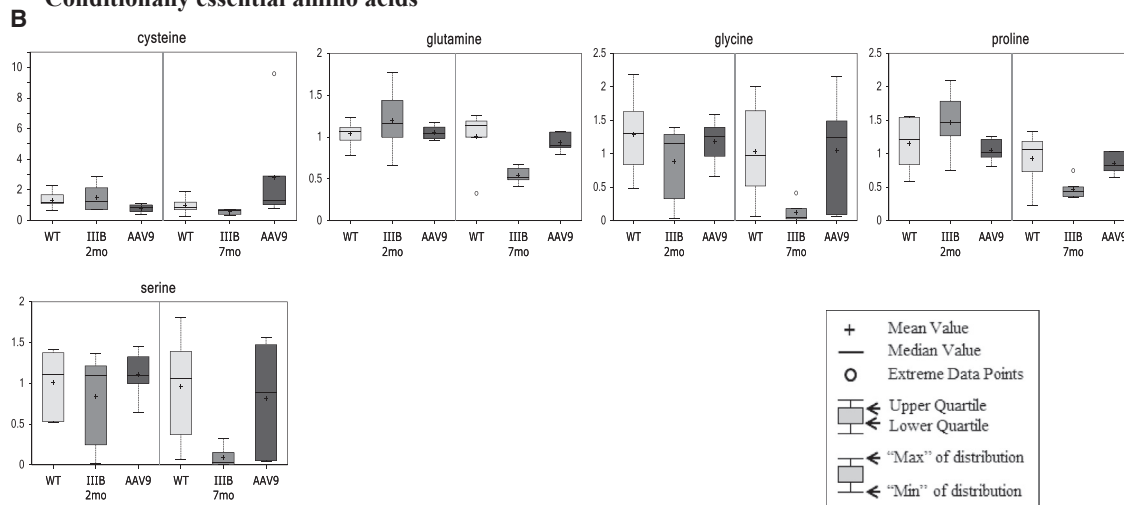
The primary pathology of MPS IIIB is lysosomal accumulation of heparan sulfate GAGs in cells of virtually all tissues/organs, especially in the CNS involving both neuronal and non-neuronal cells. While detailed mechanisms of pathology of MPS III are not yet well understood, numerous studies have reported cascades of complex secondary pathological changes in MPS IIIB.^{3,4,6,37} In this study, using metabolomic profiling of serum, we detected a severe progressive metabolic disturbance in MPS IIIB mice, which emerges early during disease progression. While previous studies reported metabolic impairments in MPS IIIB secondary to lysosomal GAG accumulation,^{3,4,6} this study demonstrates that the metabolic abnormalities in MPS IIIB mice are much more profound than previously understood, involving virtually all metabolic pathways of amino acids, peptides, lipids, carbohydrates, energy, nucleotides, vitamins and cofactors, and xenobiotics. Notably, nearly all significantly altered serum metabolites in MPS IIIB mice were predominantly reduced (97.4%), indicating that lysosomal accumulation of heparan sulfate GAGs triggers severe impairments in widespread biochemical pathways, leading to profound metabolic depression. These data further support the complexity and severity of MPS IIIB manifestations. Given the resemblance of the MPS IIIB mouse model to the human disease,³ we anticipate that the observed profound metabolic impairments in mice in this study also may occur in patients with MPS IIIB. Previous studies also showed broad metabolomic impairments in the liver in mouse models of MPS I and MPS VII,³⁸ suggesting profound metabolic abnormalities also may occur in different MPS disorders, given that these closely related diseases share many pathological features.

We also demonstrate here that the depressed amino acid metabolism in MPS IIIB mice involves the majority (virtually all) of essential, conditionally essential, and non-essential amino acids, indicating broad functional defects in amino acid (aa) metabolism, from absorption, transport, and biosynthesis to catabolism. Similar disturbances also occur in virtually all metabolism pathways, involving lipids, carbohydrates, peptides, nucleotides, energy, vitamins and cofactors, and xenobiotics. Therefore, our data offer critical information for better understanding the disease pathology and therapeutic development of MPS IIIB with regard to metabolic impairments. It is apparent that managing diet may not be feasible for achieving therapeutic benefits toward MPS IIIB. While the detailed mechanisms behind the broad metabolic impairments in MPS IIIB remain unclear, a

A Essential amino acids



B Conditionally essential amino acids



C Non-essential amino acids

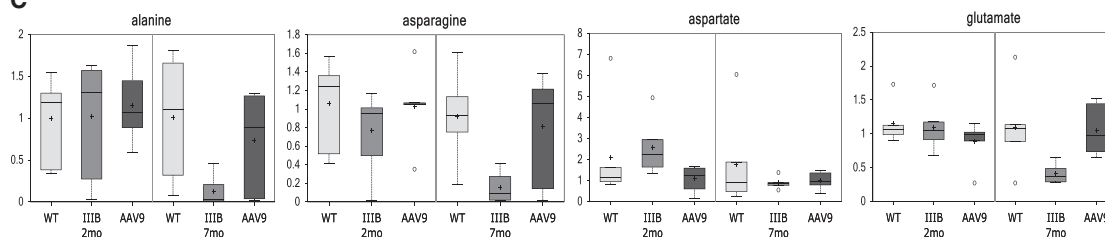


Figure 2. Impairments in Metabolism of Essential, Conditionally Essential, and Non-essential Amino Acids in MPS IIIIB Mice during Disease Progress

(A–C) Mouse serum samples were analyzed by global metabolomic profiling using mass spectrometry at the age of 2 or 7 months ($n = 6/\text{group}$). Data are presented as Scaled Intensity (y axis) using whiskers boxplots, based on $p \leq 0.05$ IIIIB-7 m versus WT-7 m. WT, wild-type mice; IIIIB, MPS IIIIB mice; AAV9, MPS IIIIB mice treated at age 1 month with an i.v. injection of 5×10^{12} vg/kg rAAV9-CMV-hNAGLU.

significant reduction in key components of the glycosylation pathway indicates the profound dysfunction of protein and lipid glycosylation. It is known that glycosylation is critical for the functionalities and

stabilities of numerous proteins, lipids, and other macromolecules, because their functional domains are usually glycosylated.³⁹ Therefore, in MPS IIIIB, the depressed glycosylation may severely

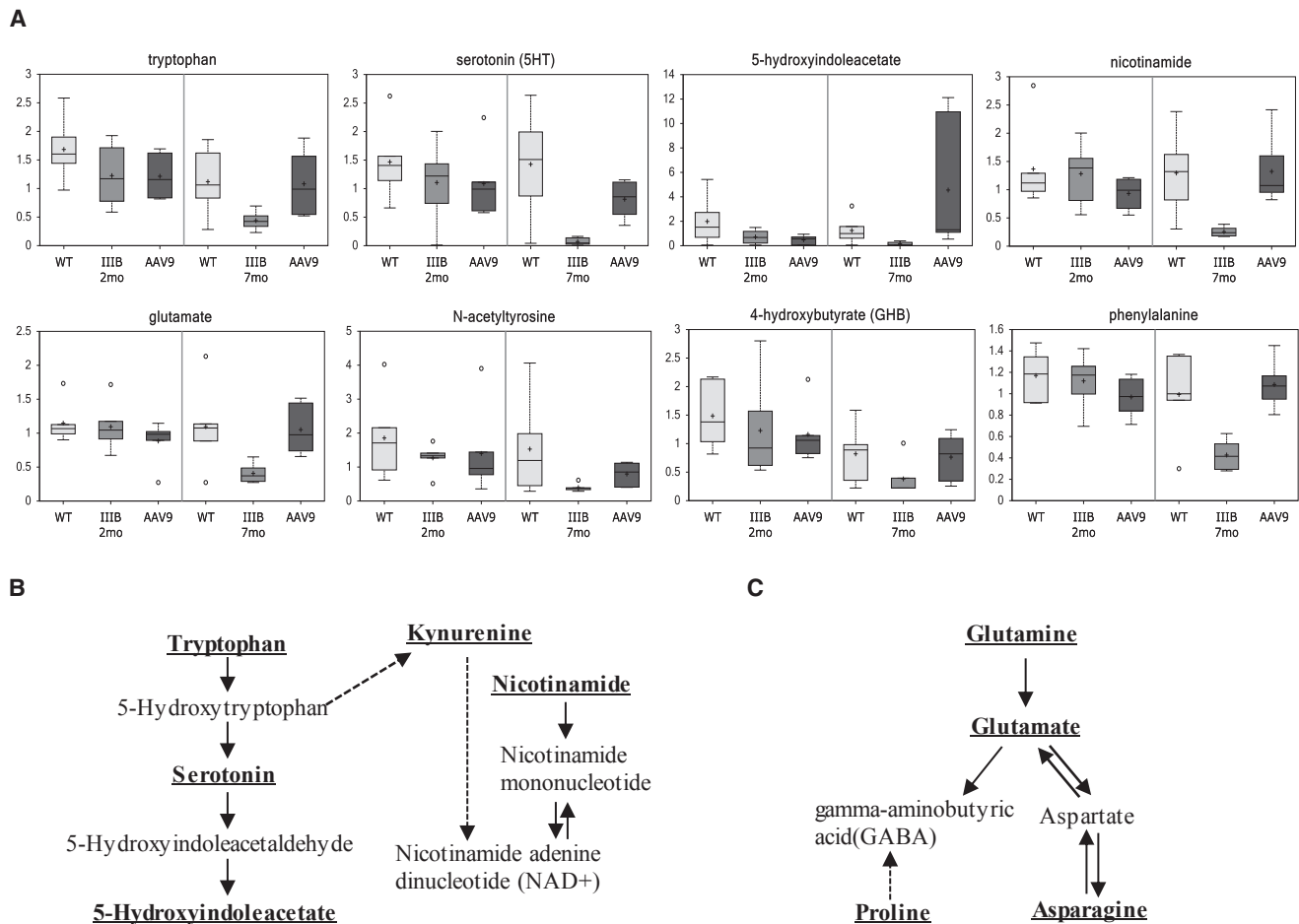


Figure 3. Abnormality in Neurotransmitter Metabolism in MPS III B during Disease Progress

Mouse serum samples were analyzed by global metabolomic profiling using mass spectrometry at the age of 2 or 7 months ($n = 6/\text{group}$). (A) Metabolomic comparison is shown; data are presented as scaled intensity (y axis) using whiskers boxplots ($p \leq 0.05$ III B-7 m versus WT-7 m). WT, wild-type mice; III B, MPS III B mice; AAV9, MPS III B mice treated at the age of 1 month with an i.v. injection of 5×10^{12} vg/kg rAAV9-CMV-hNAGLU. (B) Disturbance of serotonin and kynurenine pathway is shown. (C) Glutamate, aspartate, and the GABA pathway are shown. Bold and underlined metabolites, $p \leq 0.05$ III B-7 m versus WT-7 m.

compromise the biological functions of macromolecules, leading to such broad metabolic impairments, which may contribute to profound cell dysfunction, and severe CNS and systemic disorders.

One of the significant novel findings in this study is that the serum metabolomic profiles revealed severe depression of major neurotransmitter metabolism in MPS III B mice, involving pathways of glutamate, gamma-aminobutyric acid, aspartate, serotonin, and dopamine. In addition, there were significant reductions in multiple metabolites in the serum from MPS III B mice, such as ALC, scyllo-inositol, and NAA, which are linked to neurological functions and may play a role in neurological dysfunctions in MPS III B. Of them, ALC possesses unique neuroprotective, neuromodulatory, and neurotrophic properties.⁴⁰ Scyllo-inositol was found to reduce A β plaque in the brains in mice and reverse memory deficits and other symptoms associated with the presence of A β in the brain.⁴¹

NAA is a derivative of aspartate and the second most concentrated molecule in the brain, involved in neuronal osmosis, lipid and myelin synthesis in oligodendrocytes, synthesis of the important neurotransmitter N-acetylaspartylglutamate, and energy production in neuronal mitochondria.⁴² Previous studies also showed that reduced NAA may play a role in motor neuron loss in amyotrophic lateral sclerosis (ALS).⁴³ It is unclear whether the reduced serum levels of these metabolites are the contributors to, or consequences of, the severe neuropathy in MPS III B. However, many neurotransmitters are synthesized from simple and abundant precursors, such as amino acids, which are readily available from dietary proteins broken down by digestion and transported via blood circulation to cells in the nervous system.⁴⁴ It is, therefore, possible that the decreases in serum levels of neurotransmitters and derivatives are associated with the progressive neuropathic manifestations in MPS III B.

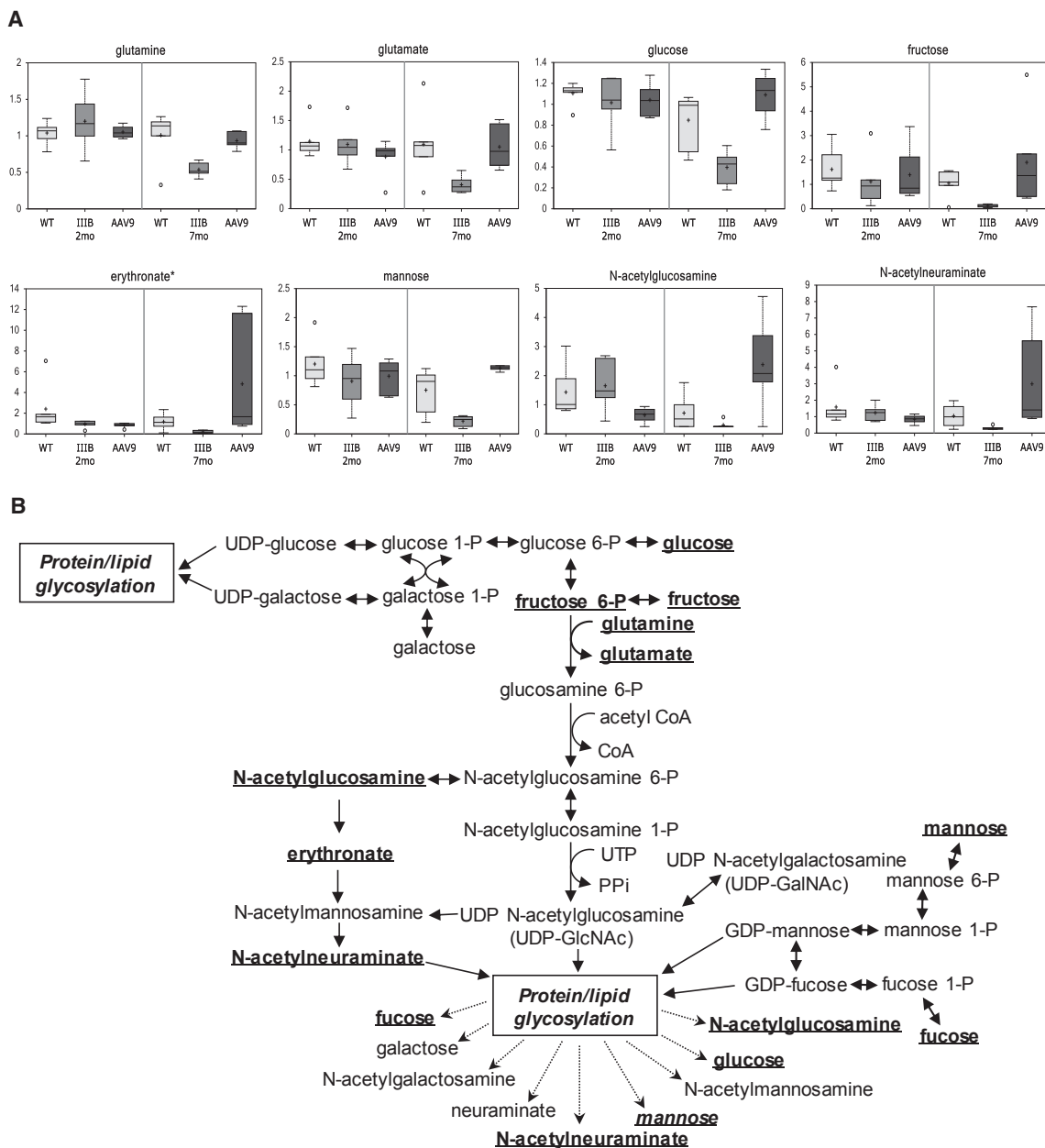


Figure 4. Broad Disturbance of Glycosylation Pathway in MPS IIIB during Disease Progress

Mouse serum samples were analyzed by global metabolomic profiling using mass spectrometry at the age of 2 or 7 months ($n = 6/\text{group}$). (A) Metabolomic comparison is shown; data are presented as scaled intensity (y axis) using whiskers boxplots ($p \leq 0.05$ IIIB-7 m versus WT-7 m). WT, wild-type mice; IIIB, MPS IIIB mice; AAV9, MPS IIIB mice treated at the age of 1 month with an i.v. injection of 5×10^{12} vg/kg rAAV9-CMV-hNAGLU. (B) Disturbance of glycosylation pathway is shown. Bold and underlined metabolites, $p \leq 0.05$ IIIB-7 m versus WT-7 m.

Most importantly, we demonstrate here that the serum metabolomic profiles in MPS IIIB mice responded well to a single systemic delivery of the rAAV9-hNAGLU, a previously established effective gene therapy approach targeting the root cause of the disease.²⁹ Notably, this systemic rAAV9-hNAGLU gene delivery approach recently has been approved by the U.S. Food and Drug Administration (FDA)

for a phase 1/2 clinical trial in MPS IIIB patients (IND 16671, to be initiated). As demonstrated previously and again in this study, a single i.v. injection of rAAV9-hNAGLU vector resulted in the efficient restoration of functional rNAGLU and clearance of GAG storage in the CNS and broad somatic tissues, as well as functional benefits, leading to behavioral correction and significantly extended survival

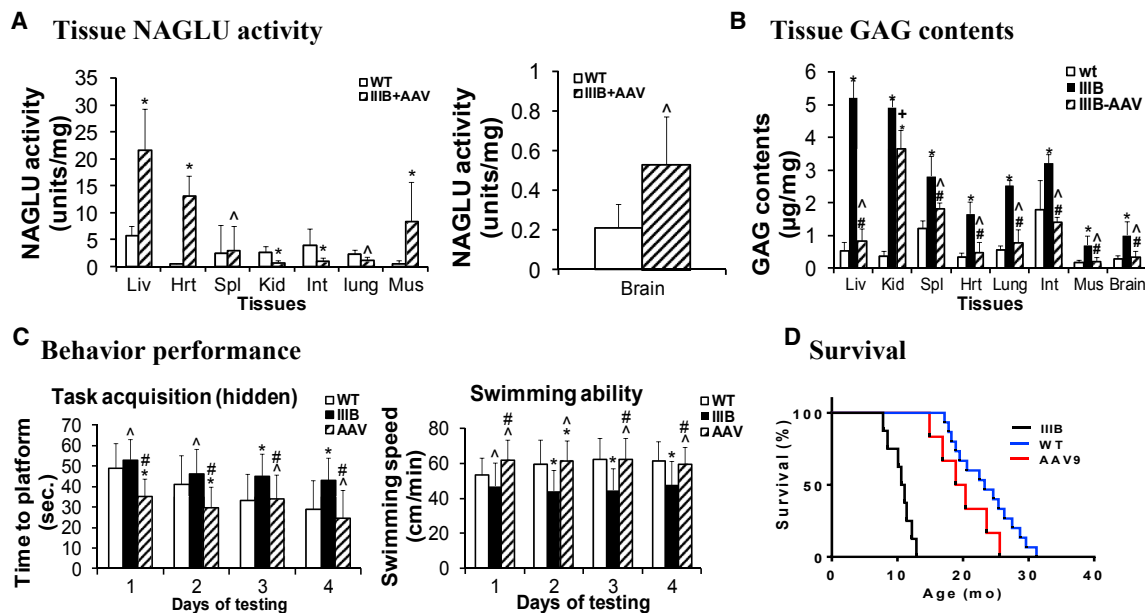


Figure 5. Restoration of Tissue NAGLU Activity, Correction of GAG Storage, Normalized Behavior, and Extended Survival in MPS IIIB Mice following a Systemic rAAV9-hNAGLU Gene Delivery

MPS IIIB mice were treated with an i.v. injection of 5×10^{12} vg/kg rAAV9-CMV-hNAGLU at the age of 1 month. Tissues ($n = 6$ /group) were assayed for NAGLU activity (A) and GAG contents (B). NAGLU activity is presented as units/mg protein (means \pm SD, 1 unit = release of nmol 4 MU/hr). GAG contents is presented as μ g/mg wet tissue (means \pm SD). The animals also were tested for behavior at the age of 5–5.5 months ($n = 13$) in a hidden task in the Morris water maze (C) and observed for longevity (D). WT, wild-type mice; IIIB, MPS IIIB mice; IIIB + AAV or AAV, AAV9-treated MPS IIIB mice. * $p \leq 0.05$ versus WT; ^ $p > 0.05$ versus WT; # $p \leq 0.05$ versus IIIB.

in MPS IIIB mice. Most importantly, the effective restoration of functional NAGLU following rAAV9-hNAGLU gene delivery treatment led to the normalization of the majority (>87%) and over-correction of 13% of the serum metabolomic abnormalities in MPS IIIB mice. This study further supports the successful functional therapeutic benefits of our systemic rAAV9-hNAGLU gene therapy approach for the treatment of both the neurological and somatic disorders of MPS IIIB, and it supports the surrogate biomarker potential of serum metabolomic signatures. We also strongly believe that serum metabolomic profiles may provide a powerful tool for studying disease mechanisms and identifying specific potential biomarkers for assessing disease progression, severity, and therapeutic outcome for MPS IIIB. Notably, previous studies showed that a single i.v. injection of recombinant iduronidase (Aldurazyme) normalized caloric density within 48 hr in MPS I mice.⁶ Furthermore, this biomarker potential of serum metabolomic profiling observed may be applicable to humans, given the resemblance of the MPS IIIB mouse model to the human disease.³ This may be more important now than ever as effective gene therapy and other therapies advance toward clinical application; since there are no effective biomarkers, especially neurological biomarkers, currently available for MPS IIIB; and due to the rarity and lack of treatments. Further efforts are needed to identify more specific and confined metabolome sets as biomarkers for MPS IIIB.

In summary, using serum global metabolomic profiling, we demonstrate here that MPS IIIB triggers broad profound metabolic impair-

ments in mice, possibly from absorption, transport, and biosynthesis, involving virtually all metabolism pathways. Serum metabolites respond well to the effective gene therapy approach and offer great surrogate biomarker potential for MPS IIIB.

MATERIALS AND METHODS

Animals

The MPS IIIB knockout mouse colony³ was maintained on an inbred background (C57BL/6) of backcrosses from heterozygotes in the vivarium at NCH-RI. All animal care and procedures were in accordance with the Guide for the Care and Use of Laboratory Animals and the protocol that was approved by the Institutional Animal Care and Use Committee at the Research Institute at Nationwide Children's Hospital. The genotypes of progeny mice were identified by PCR.

MPS IIIB mice and their age-matched WT littermates were used in the experiments, as described in the previously published manuscript.³⁷

Intravenous Injection of rAAV9-hNAGLU Viral Vector

A previously described rAAV vector plasmid was used to produce rAAV9-CMV-hNAGLU viral vector.³⁷ The vector genome contained AAV2 terminal repeats, a CMV immediate-early promoter, SV40 splice donor/acceptor signals, a human NAGLU coding sequence, and a polyadenylation signal from the bovine growth hormone

Table 3. Correction of Metabolomic Abnormalities in MPS IIIB Mice by an i.v. rAAV9-hNAGLU Gene Delivery

Groups	Age (Months)	Number of Metabolites Altered ($p \leq 0.05$)		
		Decrease	Increase	Total
IIIB/WT	2	17	1	18
AAV9/WT	2	2 ^a /6 ^b	0	8
IIIB/WT	7	225	6	231
AAV9/WT	7	1 ^b	30 ^a /27 ^b	58

At 2 and 7 months of age, serum samples were assayed by global metabolomic profiling for 361 metabolites, using mass spectrometry. IIIB, non-treated MPS IIIB mice; WT, wild-type mice; AAV9, MPS IIIB mice treated with an i.v. injection of rAAV9-CMV-hNAGLU vector (5e12 vg/kg) at the age of 1 month.

^aNumber of metabolites unchanged after vector treatment.
^bNumber of metabolites altered after vector treatment.

gene. The viral vectors were produced in HEK293 cells using three-plasmid co-transfection, including AAV helper plasmid encoding serotype 9 capsid, and purified following published procedures.⁴⁵ The rAAV9-CMV-hNAGLU vector (5×10^{12} vg/kg, in 150–200 μ L PBS) was delivered via tail vein to MPS IIIB mice at the age of 1 month.

Behavioral Tests: Hidden Task in the Morris Water Maze

The rAAV9-CMV-hNAGLU-treated MPS IIIB mice and controls were tested for behavioral performance at ~5.0–5.5 months of age in a hidden task in the Morris water maze, as previously described.^{37,46} Measures of latency were taken to find the platform, swimming distance (cm), and swimming velocity (cm/min) through an automated tracking system (San Diego Instruments).

Tissue Analyses

Necropsies were performed at 2 or 6 months of age ($n = 6$ /group, M:F = 3:3) for tissue analyses. After the mice were anesthetized with an intraperitoneal (i.p.) injection of ketamine/xylazine cocktail, blood, brain, and multiple somatic tissue samples were collected. Tissue and serum samples were stored at -80°C before being processed for analyses.

NAGLU Activity Assay

Tissue samples were assayed for NAGLU enzyme activity following published procedures.⁴⁷ The assay measures 4-methylumbelliferone, a fluorescent product formed by hydrolysis of the substrate 4-methylumbelliferyl-*N*-acetyl- α -D-glucosaminide. The NAGLU activity is expressed as unit/mg protein. One unit is equal to 1 nmol 4-methylumbelliferone released/hr at 37°C .

GAG Content Measurement

GAG was extracted from tissues following published procedures with modification.^{48,49} Dimethylmethylene blue (DMB) assay was used to measure GAG content.⁵⁰ The GAG samples (from 0.5 to 1.0 mg tissue) were mixed with H_2O to 40 μ L before adding 35 nM DMB (Polysciences) in 0.2 mmol/L sodium formate buffer (pH 3.5). The product

was measured using a spectrophotometer (OD_{535}). The GAG content was expressed as $\mu\text{g}/\text{mg}$ tissue.

Serum Sample Process for Metabolomic Analyses

Serum samples were assayed for metabolites at Metabolon. All serum samples were stored at -80°C prior to analyses. At the time of the analyses, serum samples were processed to extract metabolites using the automated MicroLab STAR system (Hamilton) and Metabolon's standard methods via a methanol extraction, allowing maximum recovery of small molecules. Each resulting serum sample extract was divided into four equal fractions, for gas chromatography-MS (GC-MS), liquid chromatography-tandem MS (LC-MS/MS) positive, LC-MS/MS negative, and one retained for backup, and they were subjected to metabolomic analyses.

Global Metabolomic Profiling

Non-targeted global metabolomic profiling (Metabolon) of mouse serum was performed using GC-MS and ultrahigh-performance LC-MS/MS (UPLC-MS/MS) as previously described,⁵¹ resulting in the identification and quantification of 361 compounds of known identity. The UPLC-MS/MS analysis platform included an LTQ mass spectrometer (Thermo Fisher Scientific) equipped with a Waters Acquity UPLC system, which consisted of an electrospray ionization (ESI) source and linear ion-trap (LIT) mass analyzer. The GC-MS analysis platform was performed on a Thermo-Finnigan Trace DSQ fast-scanning single-quadrupole mass spectrometer using electron impact ionization. The information output from the raw data files was automatically extracted, and metabolites were identified by comparison to metabolomic library entries of purified standards or recurrent unknown entities. Data are presented as fold of change in (1) MPS IIIB mice versus WT, (2) MPSIIIB at the age of 7 versus 2 months, or (3) AAV-treated versus non-treated MPS IIIB mice (>1.0 , increase; <1.0 , decrease).

Statistical Analysis

The Student's *t* test, one-way ANOVA, and Bonferroni correction were used to analyze NAGLU activity, GAG contents, and behavior data for group-to-group comparison, and significance was defined as $p \leq 0.05$. Repeated ANOVA was performed to assess group differences when combining data from all test groups. Statistical analysis of log-transformed metabolomic data was performed using Welch's *t* test, two-way ANOVA, and the false discovery rate (FDR), and significance was defined as $p \leq 0.05$ and $q \leq 0.10$.

SUPPLEMENTAL INFORMATION

Supplemental Information includes four figures and one table and can be found with this article online at <http://dx.doi.org/10.1016/j.ymthe.2016.12.025>.

AUTHOR CONTRIBUTIONS

H.F. conceived this study. H.F. and D.M.M. co-designed the experiments. A.S.M. and T.W. performed the animal experiments and data collection. R.P.M. contributed to metabolomics analyses. All authors contributed to the manuscript preparation.

CONFLICTS OF INTEREST

H.F. and D.M.M. are co-inventors of Abeona Therapeutics' ABO-101 and ABO-102.

ACKNOWLEDGMENTS

This study was supported by donations from families and friends of patients with Sanfilippo syndromes through LivLife Foundation and Regan's Hope and residue research grants from Ben's Dream – Sanfilippo Research Foundation and Cure Kirby – Children's Medical Research Foundation. H.F., A.S.M., and D.M.M. also were supported by a translational research grant from the NIH/NINDS (U01NS069626). D.M.M. and H.F. also were supported by a grant from the NIH/NCI (R01CA172713).

REFERENCES

- Neufeld, E.F., and Muenzer, J. (2001). The mucopolysaccharidoses. In *The metabolic & molecular basis of inherited disease*, Eighth Edition, C.R. Scriver, A.L. Beaudet, W.S. Sly, and D. Valle, eds. (McGraw-Hill), pp. 3421–3452.
- Yogalingam, G., and Hopwood, J.J. (2001). Molecular genetics of mucopolysaccharidosis type IIIA and IIIB: Diagnostic, clinical, and biological implications. *Hum. Mutat.* *18*, 264–281.
- Li, H.H., Yu, W.H., Rozengurt, N., Zhao, H.Z., Lyons, K.M., Anagnostaras, S., Fanselow, M.S., Suzuki, K., Vanier, M.T., and Neufeld, E.F. (1999). Mouse model of Sanfilippo syndrome type B produced by targeted disruption of the gene encoding alpha-N-acetylglucosaminidase. *Proc. Natl. Acad. Sci. USA* *96*, 14505–14510.
- McGlynn, R., Dobrenis, K., and Walkley, S.U. (2004). Differential subcellular localization of cholesterol, gangliosides, and glycosaminoglycans in murine models of mucopolysaccharide storage disorders. *J. Comp. Neurol.* *480*, 415–426.
- Wilkinson, F.L., Holley, R.J., Langford-Smith, K.J., Badrinath, S., Liao, A., Langford-Smith, A., Cooper, J.D., Jones, S.A., Wraith, J.E., Wynn, R.F., et al. (2012). Neuropathology in mouse models of mucopolysaccharidosis type I, IIIA and IIIB. *PLoS ONE* *7*, e35787.
- Woloszynek, J.C., Coleman, T., Semenkovich, C.F., and Sands, M.S. (2007). Lysosomal dysfunction results in altered energy balance. *J. Biol. Chem.* *282*, 35765–35771.
- Li, H.H., Zhao, H.Z., Neufeld, E.F., Cai, Y., and Gómez-Pinilla, F. (2002). Attenuated plasticity in neurons and astrocytes in the mouse model of Sanfilippo syndrome type B. *J. Neurosci. Res.* *69*, 30–38.
- Ohmi, K., Greenberg, D.S., Rajavel, K.S., Ryazantsev, S., Li, H.H., and Neufeld, E.F. (2003). Activated microglia in cortex of mouse models of mucopolysaccharidoses I and IIIB. *Proc. Natl. Acad. Sci. USA* *100*, 1902–1907.
- Tamagawa, K., Morimatsu, Y., Fujisawa, K., Hara, A., and Taketomi, T. (1985). Neuropathological study and chemico-pathological correlation in sibling cases of Sanfilippo syndrome type B. *Brain Dev.* *7*, 599–609.
- Villani, G.R., Gargiulo, N., Faraonion, R., Castaldo, S., Gonzalez Y Reyero, E., and Di Natale, P. (2007). Cytokines, neurotrophins, and oxidative stress in brain disease from mucopolysaccharidosis IIIB. *J. Neurosci. Res.* *85*, 612–622.
- DiRosario, J., Divers, E., Wang, C., Etter, J., Charrier, A., Jukkola, P., Auer, H., Best, V., Newsom, D.L., McCarty, D.M., and Fu, H. (2009). Innate and adaptive immune activation in the brain of MPS IIIB mouse model. *J. Neurosci. Res.* *87*, 978–990.
- Villani, G.R., Di Domenico, C., Musella, A., Cecere, F., Di Napoli, D., and Di Natale, P. (2009). Mucopolysaccharidosis IIIB: oxidative damage and cytotoxic cell involvement in the neuronal pathogenesis. *Brain Res.* *1279*, 99–108.
- Ryazantsev, S., Yu, W.H., Zhao, H.Z., Neufeld, E.F., and Ohmi, K. (2007). Lysosomal accumulation of SCMAS (subunit c of mitochondrial ATP synthase) in neurons of the mouse model of mucopolysaccharidosis III B. *Mol. Genet. Metab.* *90*, 393–401.
- Settembre, C., Fraldi, A., Jahreiss, L., Spanpanato, C., Venturi, C., Medina, D., de Pablo, R., Tacchetti, C., Rubinsztein, D.C., and Ballabio, A. (2008). A block of autophagy in lysosomal storage disorders. *Hum. Mol. Genet.* *17*, 119–129.
- Ginsberg, S.D., Galvin, J.E., Lee, V.M., Rorke, L.B., Dickson, D.W., Wolfe, J.H., Jones, M.Z., and Trojanowski, J.Q. (1999). Accumulation of intracellular amyloid-beta peptide (A beta 1-40) in mucopolysaccharidosis brains. *J. Neuropathol. Exp. Neurol.* *58*, 815–824.
- Winder-Rhodes, S.E., Garcia-Reitböck, P., Ban, M., Evans, J.R., Jacques, T.S., Kempainen, A., Foltynie, T., Williams-Gray, C.H., Chinnery, P.F., Hudson, G., et al. (2012). Genetic and pathological links between Parkinson's disease and the lysosomal disorder Sanfilippo syndrome. *Mov. Disord.* *27*, 312–315.
- Ohmi, K., Kudo, L.C., Ryazantsev, S., Zhao, H.Z., Karsten, S.L., and Neufeld, E.F. (2009). Sanfilippo syndrome type B, a lysosomal storage disease, is also a tauopathy. *Proc. Natl. Acad. Sci. USA* *106*, 8332–8337.
- Ohmi, K., Zhao, H.Z., and Neufeld, E.F. (2011). Defects in the medial entorhinal cortex and dentate gyrus in the mouse model of Sanfilippo syndrome type B. *PLoS ONE* *6*, e27461.
- Hamano, K., Hayashi, M., Shioda, K., Fukatsu, R., and Mizutani, S. (2008). Mechanisms of neurodegeneration in mucopolysaccharidoses II and IIIB: analysis of human brain tissue. *Acta Neuropathol.* *115*, 547–559.
- Kurihara, M., Kumagai, K., and Yagishita, S. (1996). Sanfilippo syndrome type C: a clinicopathological autopsy study of a long-term survivor. *Pediatr. Neurol.* *14*, 317–321.
- Huang, Y., and Mucke, L. (2012). Alzheimer mechanisms and therapeutic strategies. *Cell* *148*, 1204–1222.
- McCarty, D.M., DiRosario, J., Gulaid, K., Killedar, S., Oosterhof, A., van Kuppevelt, T.H., Martin, P.T., and Fu, H. (2011). Differential distribution of heparan sulfate glycoforms and elevated expression of heparan sulfate biosynthetic enzyme genes in the brain of mucopolysaccharidosis IIIB mice. *Metab. Brain Dis.* *26*, 9–19.
- Kumar, K.R., Djarmati-Westenberger, A., and Grünewald, A. (2011). Genetics of Parkinson's disease. *Semin. Neurol.* *31*, 433–440.
- Panaro, M.A., and Cianciulli, A. (2012). Current opinions and perspectives on the role of immune system in the pathogenesis of Parkinson's disease. *Curr. Pharm. Des.* *18*, 200–208.
- Fu, H., Bartz, J.D., Stephens, R.L., Jr., and McCarty, D.M. (2012). Peripheral nervous system neuropathology and progressive sensory impairments in a mouse model of Mucopolysaccharidosis IIIB. *PLoS ONE* *7*, e45992.
- Valayannopoulos, V., and Wijburg, F.A. (2011). Therapy for the mucopolysaccharidoses. *Rheumatology (Oxford)* *50* (Suppl 5), v49–v59.
- Byrne, B.J., Falk, D.J., Clément, N., and Mah, C.S. (2012). Gene therapy approaches for lysosomal storage disease: next-generation treatment. *Hum. Gene Ther.* *23*, 808–815.
- High, K.A., and Aubourg, P. (2011). rAAV human trial experience. *Methods Mol. Biol.* *807*, 429–457.
- Fu, H., DiRosario, J., Killedar, S., Zaraspe, K., and McCarty, D.M. (2011). Correction of neurological disease of mucopolysaccharidosis IIIB in adult mice by rAAV9 trans-blood-brain barrier gene delivery. *Mol. Ther.* *19*, 1025–1033.
- Marmiroli, P., Rodriguez-Menendez, V., Rigamonti, L., Tonoli, E., Rigolio, R., Cavaletti, G., Tredici, G., and Vercelli, A. (2009). Neuropathological changes in the peripheral nervous system and spinal cord in a transgenic mouse model of Niemann-Pick disease type A. *Clin. Neuropathol.* *28*, 263–274.
- Duque, S., Joussemet, B., Riviere, C., Marais, T., Dubreil, L., Douar, A.M., Fyfe, J., Moullier, P., Colle, M.A., and Barkats, M. (2009). Intravenous administration of self-complementary AAV9 enables transgene delivery to adult motor neurons. *Mol. Ther.* *17*, 1187–1196.
- Foust, K.D., Nurre, E., Montgomery, C.L., Hernandez, A., Chan, C.M., and Kaspar, B.K. (2009). Intravascular AAV9 preferentially targets neonatal neurons and adult astrocytes. *Nat. Biotechnol.* *27*, 59–65.
- Foust, K.D., Wang, X., McGovern, V.L., Braun, L., Bevan, A.K., Haidet, A.M., Le, T.T., Morales, P.R., Rich, M.M., Burghes, A.H., and Kaspar, B.K. (2010). Rescue of the spinal muscular atrophy phenotype in a mouse model by early postnatal delivery of SMN. *Nat. Biotechnol.* *28*, 271–274.
- Randall, D.R., Colobong, K.E., Hemmelgarn, H., Sinclair, G.B., Hetty, E., Thomas, A., Bodamer, O.A., Volkmar, B., Fernhoff, P.M., Casey, R., et al. (2008). Heparin cofactor II-thrombin complex: a biomarker of MPS disease. *Mol. Genet. Metab.* *94*, 456–461.

35. Beesley, C.E., Young, E.P., Finnegan, N., Jackson, M., Mills, K., Vellodi, A., Cleary, M., and Winchester, B.G. (2009). Discovery of a new biomarker for the mucopolysaccharidoses (MPS), dipeptidyl peptidase IV (DPP-IV; CD26), by SELDI-TOF mass spectrometry. *Mol. Genet. Metab.* 96, 218–224.
36. Lawrence, R., Brown, J.R., Al-Mafraji, K., Lamanna, W.C., Beitel, J.R., Boons, G.J., Esko, J.D., and Crawford, B.E. (2012). Disease-specific non-reducing end carbohydrate biomarkers for mucopolysaccharidoses. *Nat. Chem. Biol.* 8, 197–204.
37. Naughton, B.J., Duncan, F.J., Murrey, D., Ware, T., Meadows, A., McCarty, D.M., and Fu, H. (2013). Amyloidosis, synucleinopathy, and prion encephalopathy in a neuro-pathic lysosomal storage disease: the CNS-biomarker potential of peripheral blood. *PLoS ONE* 8, e80142.
38. Woloszynek, J.C., Kovacs, A., Ohlemiller, K.K., Roberts, M., and Sands, M.S. (2009). Metabolic adaptations to interrupted glycosaminoglycan recycling. *J. Biol. Chem.* 284, 29684–29691.
39. Varki, A., Sharon, N., Bertozzi, C.R., Rabuka, D., Esko, J.D., Colley, K.J., Freeze, H.H., Elbein, A.D., Rini, J., Lowe, J.B., et al. (2009). General principles. In *Essentials of Glycobiology*, Second Edition, A. Varki, R.D. Cummings, J.D. Esko, H.H. Freeze, P. Stanley, C.R. Bertozzi, G.W. Hart, and M.E. Etzler, eds. (Cold Spring Harbor Laboratory Press).
40. Virmani, A., and Binienda, Z. (2004). Role of carnitine esters in brain neuropathology. *Mol. Aspects Med.* 25, 533–549.
41. McLaurin, J., Kierstead, M.E., Brown, M.E., Hawkes, C.A., Lambermon, M.H., Phinney, A.L., Darabie, A.A., Cousins, J.E., French, J.E., Lan, M.F., et al. (2006). Cyclohexanehexol inhibitors of Abeta aggregation prevent and reverse Alzheimer phenotype in a mouse model. *Nat. Med.* 12, 801–808.
42. Moffett, J.R., Ross, B., Arun, P., Madhavao, C.N., and Namboodiri, A.M. (2007). N-Acetylaspartate in the CNS: from neurodiagnostics to neurobiology. *Prog. Neurobiol.* 81, 89–131.
43. Rothstein, J.D., Tsai, G., Kuncl, R.W., Clawson, L., Cornblath, D.R., Drachman, D.B., Pestronk, A., Stauch, B.L., and Coyle, J.T. (1990). Abnormal excitatory amino acid metabolism in amyotrophic lateral sclerosis. *Ann. Neurol.* 28, 18–25.
44. Deutch, A.Y., and Roth, R.H. (2003). Neurotransmitters. In *Fundamental Neuroscience*, Second Edition, L.R. Squire, F.E. Bloom, S.K. McConnell, J.L. Roberts, N.C. Spitzer, and M.J. Zigmond, eds. (San Diego: Academic Press), pp. 163–196.
45. Zolotukhin, S., Byrne, B.J., Mason, E., Zolotukhin, I., Potter, M., Chesnut, K., Summerford, C., Samulski, R.J., and Muzyczka, N. (1999). Recombinant adeno-associated virus purification using novel methods improves infectious titer and yield. *Gene Ther.* 6, 973–985.
46. Warburton, E.C., Baird, A., Morgan, A., Muir, J.L., and Aggleton, J.P. (2001). The conjoint importance of the hippocampus and anterior thalamic nuclei for allocentric spatial learning: evidence from a disconnection study in the rat. *J. Neurosci.* 21, 7323–7330.
47. Thompson, J.N., and Nowakowski, R.W. (1991). Enzymatic diagnosis of selected mucopolysaccharidoses: Hunter, Morquio type A, and Sanfilippo types A, B, C, and D, and procedures for measurement of 35SO₄-glycosaminoglycans. In *Techniques in diagnostic human biochemical genetics - a laboratory manual*, F.A. Hommes, ed. (Wiley-Liss), pp. 567–586.
48. van de Lest, C.H., Versteeg, E.M., Veerkamp, J.H., and van Kuppevelt, T.H. (1994). Quantification and characterization of glycosaminoglycans at the nanogram level by a combined azure A-silver staining in agarose gels. *Anal. Biochem.* 221, 356–361.
49. Fu, H., Kang, L., Jennings, J.S., Moy, S.S., Perez, A., Dirosario, J., McCarty, D.M., and Muenzer, J. (2007). Significantly increased lifespan and improved behavioral performances by rAAV gene delivery in adult mucopolysaccharidosis IIIB mice. *Gene Ther.* 14, 1065–1077.
50. de Jong, J.G., Wevers, R.A., Laarakkers, C., and Poorthuis, B.J. (1989). Dimethylmethylene blue-based spectrophotometry of glycosaminoglycans in untreated urine: a rapid screening procedure for mucopolysaccharidoses. *Clin. Chem.* 35, 1472–1477.
51. Sekula, P., Goek, O.N., Quaye, L., Barrios, C., Levey, A.S., Römisch-Margl, W., Menni, C., Yet, L., Gieger, C., Inker, L.A., et al. (2016). A metabolome-wide association study of kidney function and disease in the general population. *J. Am. Soc. Nephrol.* 27, 1175–1188.

YMTHE, Volume 25

Supplemental Information

Near-Complete Correction of Profound Metabolomic Impairments Corresponding to Functional Benefit in MPS IIIB Mice after IV rAAV9-hNAGLU Gene Delivery

Haiyan Fu, Aaron S. Meadows, Tierra Ware, Robert P. Mohny, and Douglas M. McCarty

Supplementary Table S1 Metabolomic impairments in MPS IIB mice and their responses to an IV injection of rAAV8-CMV-hNAGLU vector									
Pathways	Sub-pathways	Metabolites	Fold of Change						
			IIB-2m WT-2m	IIB-7m WT-7m	AAV9-2m WT-2m	AAV9-7m WT-7m	WT-7m WT-2m	IIB-7m IIB-2m	AAV9-7m AAV9-2m
Amino Acid	Glycine, Serine and Threonine Metabolism	glycine	0.69	0.11	0.92	1.01	0.8	0.13	0.88
		N-acetylglycine	0.43	0.12	0.64	1.3	0.68	0.19	1.39
		sarcosine (N-Methylglycine)	1.22	2.44	0.77	0.86	0.9	1.81	1.01
		dimethylglycine	0.99	0.4	0.77	1.84	0.65	0.26	1.55
		betaine	0.99	0.84	1.13	0.85	0.9	0.77	0.67
		serine	0.83	0.09	1.09	0.85	0.95	0.11	0.74
		N-acetylserine	0.74	0.29	0.52	3.6	0.53	0.21	3.69
		beta-hydroxypyruvate	1.22	0.59	0.99	1.15	0.86	0.42	1
	threonine	1.45	1.11	0.6	1.47	0.76	0.58	1.85	
	Alanine and Aspartate Metabolism	alanine	1.03	0.13	1.17	0.72	1.02	0.12	0.63
		N-acetylanaline	1.01	0.28	0.73	1.2	0.89	0.25	1.47
		aspartate	1.23	0.51	0.52	0.56	0.84	0.35	0.91
		asparagine	0.73	0.16	0.98	0.88	0.87	0.2	0.79
		N-acetylaspartate (NAA)	1.02	0.21	0.84	1.54	1.01	0.21	1.83
	Glutamate Metabolism	glutamate	0.95	0.37	0.77	0.96	0.96	0.37	1.19
		glutamine	1.15	0.53	1.01	0.92	0.97	0.45	0.89
		N-acetylglutamate	0.47	0.43	0.29	3.46	0.56	0.51	6.54
		N-acetylglutamine	0.45	0.3	0.44	2.47	0.66	0.45	3.69
	Histidine Metabolism	histidine	0.95	0.47	0.94	1.09	0.89	0.45	1.04
		N-acetylhistidine	0.49	0.18	0.5	1.68	0.68	0.25	2.28
		trans-urocanate	1.06	0.2	0.97	0.72	1.52	0.28	1.12
		cis-urocanate	0.81	0.33	0.76	1.2	1.17	0.47	1.85
		imidazole propionate	0.55	0.64	0.32	3.06	0.58	0.68	5.53
		1-methylimidazoleacetate	0.74	0.26	0.53	2.57	0.87	0.31	4.26
	Lysine Metabolism	lysine	0.77	0.18	0.68	0.61	0.67	0.16	0.6
		2-aminoadipate	1.08	0.99	0.61	1.27	0.66	0.61	1.4
		pipecolate	0.98	0.5	0.89	2.83	0.77	0.4	2.46
		5-aminovalerate	1.53	0.9	1.01	2.02	0.91	0.53	1.82
	Phenylalanine and Tyrosine Metabolism	phenylalanine	0.96	0.43	0.83	1.09	0.85	0.38	1.12
		N-acetylphenylalanine	0.9	0.33	0.87	0.99	0.86	0.32	0.97
phenyllactate (PLA)		1.23	0.58	0.93	1.85	1.03	0.48	2.04	

	phenylacetate	1	0.49	0.99	1.05	0.64	0.31	0.68
	phenylacetylglycine	0.34	0.23	0.25	6.55	0.42	0.29	10.89
	tyrosine	1.12	0.72	1.03	0.82	0.94	0.6	0.75
	N-acetyltyrosine	0.68	0.26	0.75	0.52	0.82	0.31	0.57
	4-hydroxycinnamate	0.25	0.25	0.22	0.38	0.66	<i>0.64</i>	1.12
	4-hydroxyphenylpyruvate	0.81	0.79	0.77	1.53	0.73	0.71	1.46
	3-(4-hydroxyphenyl)lactate	1.1	0.41	0.94	1.32	0.98	0.36	1.37
	phenol sulfate	0.46	0.31	0.46	2.61	0.52	0.34	2.94
	p-cresol sulfate	0.87	0.26	0.73	3.18	0.82	0.24	3.54
	2-amino-p-cresol sulfate	0.15	0.47	0.24	6.24	0.31	0.97	8.2
	homovanillate sulfate	0.28	0.46	0.22	6.65	0.41	0.67	12.4
	phenylpropionylglycine	0.44	0.23	0.59	2.71	0.95	0.49	4.39
	2-(4-hydroxyphenyl)propionate	0.7	0.53	0.39	9.94	0.62	0.46	15.7
	3-phenylpropionate (hydrocinnamate)	1.01	0.6	1.42	0.36	1.15	0.69	0.29
Tryptophan Metabolism	tryptophan	0.73	0.39	0.72	0.97	0.66	0.36	0.89
	N-acetyltryptophan	0.58	0.26	0.64	1.18	0.55	0.24	1
	indolelactate	0.63	0.18	0.45	4.26	0.56	0.16	5.37
	indolepropionate	1.79	0.79	1.8	1.63	0.59	0.26	0.53
	3-indoxyl sulfate	0.92	0.64	0.69	2.8	0.65	0.46	2.66
	kynurenine	0.61	0.26	0.6	0.98	0.74	0.32	1.21
	kynurenate	0.32	0.62	0.31	3.25	0.54	1.06	5.67
	xanthurenate	0.15	0.36	0.14	3.93	0.47	1.15	13.47
	5-hydroxyindoleacetate	0.36	0.12	0.24	3.65	0.63	0.21	9.49
	serotonin (5HT)	0.75	0.05	0.74	0.57	0.97	0.06	0.75
	C-glycosyltryptophan	0.9	0.24	0.62	3.11	0.65	0.17	3.26
Leucine, Isoleucine and Valine Metabolism	leucine	1	0.39	0.77	1	0.83	0.33	1.08
	N-acetylleucine	1.01	0.46	0.8	1.05	0.86	0.39	1.12
	4-methyl-2-oxopentanoate	0.46	0.37	0.63	0.65	0.64	0.51	0.67
	isovalerate	0.64	0.28	0.6	0.58	0.66	0.29	0.64
	isovalerylglycine	0.3	0.28	0.26	6.33	0.38	0.36	9.34
	isovalerylcarnitine	1.13	0.49	0.74	1.06	0.78	0.34	1.1
	3-methylcrotonylglycine	0.33	0.45	0.24	4.2	0.51	0.69	8.78
	beta-hydroxyisovalerate	0.74	0.25	0.7	2.46	0.66	0.22	2.32
	beta-hydroxyisovaleroylcarnitine	1.13	0.51	0.98	1.42	0.77	0.35	1.11

		alpha-hydroxyisovalerate	1.01	0.54	1.22	1.05	0.83	0.45	0.71
		isoleucine	0.83	0.38	0.78	0.94	0.8	0.37	0.97
		3-methyl-2-oxovalerate	0.33	0.39	0.65	0.69	0.61	0.72	0.64
		2-methylbutyrylcarnitine (C5)	1.31	0.55	0.67	1.61	0.63	0.27	1.52
		2-methylbutyrylglycine	0.44	0.45	0.38	3.41	0.65	0.66	5.8
		tigloylglycine	0.48	0.5	0.37	2.44	0.53	0.55	3.49
		2-hydroxy-3-methylvalerate	0.82	0.53	0.79	1.46	0.68	0.44	1.27
		valine	0.81	0.41	0.77	0.93	0.85	0.43	1.03
		3-methyl-2-oxobutyrate	0.43	0.41	0.71	0.81	0.76	0.71	0.86
		isobutyrylcarnitine	2.25	0.63	1.16	1.93	0.8	0.23	1.34
		3-hydroxyisobutyrate	0.75	0.47	0.72	0.83	0.63	0.4	0.74
		alpha-hydroxyisocaproate	0.81	0.54	0.8	0.97	0.84	0.55	1.02
	Methionine, Cysteine, SAM and Taurine Metabolism	methionine	1.21	0.64	1	0.97	0.84	0.45	0.81
		N-acetylmethionine	1.28	0.65	0.96	1.34	0.6	0.31	0.84
		N-formylmethionine	0.73	0.29	0.47	2.41	0.6	0.24	3.1
		2-aminobutyrate	0.93	0.42	0.9	1.09	0.88	0.4	1.06
		2-hydroxybutyrate (AHB)	0.57	0.2	0.62	0.89	0.81	0.29	1.17
		cysteine	1.11	0.59	0.6	2.91	0.73	0.39	3.56
		cystine	1	1.56	1	1.88	1	1.56	1.88
		taurine	1.12	0.44	0.39	1.91	0.99	0.39	4.88
	Urea cycle; Arginine and Proline Metabolism	arginine	1.27	0.98	1.61	1.04	1.22	0.94	0.79
		urea	0.93	0.56	0.68	2.38	0.65	0.39	2.29
		ornithine	0.99	0.16	0.53	0.35	0.75	0.12	0.49
		proline	1.27	0.51	0.9	0.92	0.81	0.32	0.82
		citrulline	1.03	0.87	0.87	1.52	0.73	0.61	1.27
		N-alpha-acetylornithine	1.23	0.46	0.97	1.41	0.59	0.22	0.85
		trans-4-hydroxyproline	1.1	0.2	1.17	0.78	0.61	0.11	0.41
	pro-hydroxy-pro	0.64	0.25	0.61	2.93	0.35	0.14	1.71	
	Creatine Metabolism	creatine	1.04	0.23	0.71	0.74	1.08	0.24	1.12
		creatinine	0.55	0.73	0.5	2.43	0.66	0.89	3.23
	Polyamine Metabolism	spermidine	1.63	0.9	0.8	2.34	0.98	0.54	2.88
		5-methylthioadenosine (MTA)	0.67	0.5	0.58	2.84	0.6	0.45	2.93
	Guanidino and Acetamido Metabolism	4-guanidinobutanoate	0.67	0.59	0.28	5.96	0.44	0.39	9.3

	Glutathione Metabolism	glutathione, oxidized (GSSG)	1.39	0.56	0.61	1.48	0.71	0.28	1.71
		cysteine-glutathione disulfide	1.32	0.6	0.81	2.2	0.69	0.31	1.86
		S-methylglutathione	0.65	0.62	0.21	2.61	0.29	0.28	3.66
		5-oxoproline	1.02	0.39	0.76	0.96	0.94	0.36	1.19
Peptide	Gamma-glutamyl Amino Acid	gamma-glutamylalanine	1.13	0.84	1.26	1.59	0.55	0.41	0.7
		gamma-glutamylglutamate	1.19	0.45	0.89	1.01	1.15	0.43	1.3
		gamma-glutamylisoleucine*	0.84	0.78	0.85	1.24	0.79	0.73	1.15
		gamma-glutamylleucine	1	0.49	0.7	1.24	0.61	0.3	1.08
		gamma-glutamylphenylalanine	0.98	0.62	0.77	1.52	0.55	0.34	1.09
		gamma-glutamylthreonine*	0.93	0.59	0.73	1.42	0.71	0.46	1.38
		gamma-glutamyltryptophan	1.01	0.47	0.74	1.45	0.72	0.34	1.43
		gamma-glutamyltyrosine	1.23	0.81	0.97	1.01	0.65	0.42	0.67
		gamma-glutamylvaline	0.74	0.4	0.73	1.57	0.63	0.34	1.35
	Dipeptide Derivative	anserine	0.87	0.4	0.59	0.64	1.65	0.76	1.77
	Dipeptide	alanylalanine	0.56	0.27	0.8	1.38	0.69	0.33	1.19
		alpha-glutamylalanine	1.08	1.18	0.97	0.97	1.16	1.26	1.16
	Polypeptide	bradykinin	1	1.17	1	1	1	1.17	1
	Fibrinogen Cleavage Peptide	TDTEDKGEFLSEGGGV*	0.86	0	0.96	0.83	0.91	0	0.79
TDTEDKGEFLSEGGGVR*		2.22	0.45	1.16	5.09	0.82	0.17	3.61	
Carbohydrate	Glycolysis, Gluconeogenesis, and Pyruvate Metabolism	1,5-anhydroglucitol (1,5-AG)	0.8	0.28	0.7	1.26	0.82	0.29	1.49
		glucose	0.92	0.47	0.94	1.29	0.77	0.39	1.05
		fructose-6-phosphate	1.02	0.18	0.43	1.1	1.19	0.21	3.05
		2,3-diphosphoglycerate	0.79	5.57	0.75	1.07	1.01	7.12	1.45
		3-phosphoglycerate	1.1	0.66	0.48	0.77	1.32	0.79	2.1
		phosphoenolpyruvate (PEP)	1.14	0.45	0.54	0.91	1.15	0.45	1.95
		pyruvate	0.78	1.3	1.38	0.97	0.95	1.59	0.67
		lactate	1.37	0.74	1.12	0.97	0.9	0.49	0.77
		glycerate	0.76	0.22	0.77	1.1	0.77	0.23	1.1
	Pentose Phosphate Pathway	sedoheptulose-7-phosphate	1.81	0.24	0.49	1.11	1.84	0.25	4.14
		ribulose/xylulose 5-phosphate	1.1	0.13	0.5	0.91	0.88	0.1	1.6
	Pentose Metabolism	ribulose	0.93	0.2	0.9	1.06	0.72	0.15	0.84
		ribose	0.56	0.19	0.92	0.64	0.63	0.21	0.44
		ribitol	0.57	0.35	0.67	1.54	0.8	0.49	1.83
		xylonate	0.41	0.33	0.31	6.97	0.44	0.36	10.04

		xylose	0.77	1.33	0.32	9.55	0.38	0.66	11.46
		xylitol	0.81	0.29	0.53	1.56	0.58	0.21	1.73
		threitol	0.88	0.79	0.39	6.94	0.4	0.36	7.12
		arabitol	0.67	0.24	0.35	7.66	0.41	0.14	8.78
		fucose	0.4	0.21	0.41	6.12	0.47	0.25	7.01
	Fructose, Mannose and Galactose Metabolism	fructose	0.69	0.12	0.86	1.82	0.65	0.11	1.37
		sorbitol	0.81	0.27	0.71	1.92	0.65	0.22	1.76
		mannose	0.75	0.29	0.83	1.5	0.63	0.24	1.14
		mannitol	0.93	0.57	0.49	15.4	1.04	0.64	32.57
	Aminosugar Metabolism	N-acetylglucosamine	1.15	0.43	0.45	3.33	0.5	0.18	3.69
		N-acetylneuraminate	0.78	0.3	0.53	2.87	0.66	0.25	3.54
		erythronate*	0.39	0.17	0.35	4.1	0.49	0.21	5.71
	Advanced Glycation End-product	erythrulose	0.94	0.49	0.74	1.8	0.67	0.34	1.62
Energy	TCA Cycle	citrate	0.82	0.48	0.72	4.18	0.79	0.47	4.58
		cis-aconitate	0.89	0.79	0.85	1.74	0.88	0.78	1.8
		alpha-ketoglutarate	0.51	0.29	1.11	1.15	3.21	1.85	3.34
		succinylcarnitine	0.93	0.29	0.7	1.22	1.18	0.36	2.04
		succinate	6.65	0.44	1.23	0.84	2.34	0.15	1.59
		fumarate	1.2	0.42	0.83	1.33	0.97	0.34	1.56
		malate	1.5	0.33	0.9	0.9	1.23	0.27	1.23
	Oxidative Phosphorylation	pyrophosphate (PPi)	0.83	0.62	0.85	0.42	1.24	0.93	0.61
		phosphate	1.22	1.76	0.74	0.62	1.36	1.96	1.14
Lipid	Medium Chain Fatty Acid	caproate (6:0)	0.5	0.54	0.58	1.01	0.62	0.67	1.09
		heptanoate (7:0)	0.57	0.52	0.84	1.08	0.87	0.8	1.12
		caprylate (8:0)	0.67	0.46	0.76	0.94	0.85	0.58	1.06
		pelargonate (9:0)	0.78	0.46	0.93	1.06	1.14	0.67	1.29
		caprate (10:0)	0.8	0.6	0.92	0.97	1.04	0.77	1.1
		undecanoate (11:0)	0.91	1.07	0.86	1.01	1	1.17	1.18
		laurate (12:0)	0.75	0.52	0.89	0.85	0.98	0.69	0.94
	Long Chain Fatty Acid	myristate (14:0)	0.62	0.28	0.88	0.67	1.01	0.46	0.77
		myristoleate (14:1n5)	0.51	0.1	0.82	0.54	1.17	0.22	0.77
		pentadecanoate (15:0)	0.87	0.33	0.79	0.97	1.09	0.41	1.33
		palmitate (16:0)	0.82	0.28	0.93	1.08	0.9	0.31	1.06
		palmitoleate (16:1n7)	0.5	0.15	0.67	0.63	1.06	0.33	1

		margarate (17:0)	0.89	0.3	0.94	1.13	0.95	0.32	1.14
		10-heptadecenoate (17:1n7)	0.64	0.16	0.84	0.71	1.17	0.29	0.98
		stearate (18:0)	0.93	0.37	1.01	1.32	0.83	0.33	1.09
		oleate (18:1n9)	0.65	0.14	0.74	0.91	0.97	0.22	1.18
		cis-vaccenate (18:1n7)	0.62	0.23	0.94	0.94	1.07	0.4	1.07
		nonadecanoate (19:0)	1.05	0.42	1.3	1.32	0.97	0.38	0.98
		10-nonadecenoate (19:1n9)	0.64	0.14	0.92	0.7	1.07	0.23	0.8
		arachidate (20:0)	1.19	0.61	1.1	1.53	0.75	0.38	1.04
		eicosenoate (20:1n9 or 11)	0.94	0.19	1.22	1.06	0.99	0.2	0.86
	Polyunsaturated Fatty Acid (n3 and n6)	stearidonate (18:4n3)	0.7	0.16	0.68	0.86	0.73	0.17	0.93
		eicosapentaenoate (EPA; 20:5n3)	0.65	0.27	1.04	1.09	0.94	0.38	0.99
		docosapentaenoate (n3 DPA; 22:5n3)	0.8	0.22	0.96	1.12	0.82	0.22	0.96
		docosahexaenoate (DHA; 22:6n3)	0.82	0.21	1.12	1.49	0.92	0.23	1.22
		linoleate (18:2n6)	0.84	0.19	0.85	0.9	0.97	0.22	1.04
		linolenate [alpha or gamma; (18:3n3 or 6)]	0.79	0.12	0.83	0.85	0.91	0.14	0.94
		dihomo-linolenate (20:3n3 or n6)	0.96	0.33	1.07	1.45	0.79	0.27	1.07
		arachidonate (20:4n6)	0.87	0.21	1.03	1.66	0.9	0.22	1.46
		adrenate (22:4n6)	1.25	0.38	0.96	1.23	0.94	0.29	1.2
		docosapentaenoate (n6 DPA; 22:5n6)	0.94	0.19	1.2	1.81	0.84	0.17	1.25
		docosadienoate (22:2n6)	1.58	0.48	1.55	1.45	0.87	0.27	0.82
		dihomo-linoleate (20:2n6)	0.85	0.21	1.04	1.18	0.8	0.2	0.91
		mead acid (20:3n9)	0.81	0.26	0.88	1.35	0.84	0.26	1.29
	Fatty Acid, Branched	15-methylpalmitate (isobar with 2-methylpalmitate)	0.73	0.48	0.96	0.89	1.09	0.72	1
		17-methylstearate	0.7	0.24	1.25	0.9	0.98	0.34	0.71
	Fatty Acid, Dicarboxylate	2-hydroxyglutarate	0.8	0.19	0.53	5.36	1.11	0.27	11.29
		azelate (nonanedioate)	0.86	0.69	0.68	1.29	0.83	0.66	1.57
		tetradecanedioate	0.76	0.28	0.87	0.83	1.26	0.46	1.2
		hexadecanedioate	0.81	0.16	0.99	0.82	1.15	0.22	0.95
		octadecanedioate	0.78	0.24	1.12	0.73	1.14	0.34	0.74
	Fatty Acid, Amide	stearamide	0.73	0.58	0.58	1.41	0.66	0.52	1.61
	Fatty Acid Metabolism (also BCAA Metabolism)	butyrylcarnitine	1.46	0.61	1.03	1.27	0.87	0.37	1.06
		butyrylglycine	0.2	0.19	0.23	4.43	0.39	0.37	7.68
		propionylcarnitine	1.72	1.07	0.97	0.88	1.09	0.68	0.99
	Fatty Acid Metabolism	valerylglycine	0.39	0.37	0.38	3.4	0.55	0.52	4.97

(Acyl Glycine)	hexanoylglycine	0.12	0.05	0.22	1.29	0.53	0.24	3.06
Fatty Acid Metabolism(Acyl Carnitine)	acetylcarnitine	0.9	0.37	0.88	0.9	0.91	0.38	0.94
	hexanoylcarnitine	1.05	0.26	0.9	0.93	0.84	0.21	0.86
	octanoylcarnitine	0.9	0.42	0.71	1.02	0.88	0.41	1.26
	decanoylcarnitine	0.9	0.54	0.81	0.78	0.78	0.47	0.76
	laurylcarnitine	0.38	0.58	0.69	1.18	0.5	0.76	0.85
	myristoylcarnitine	0.42	0.23	0.52	0.94	0.47	0.25	0.85
	palmitoylcarnitine	0.44	0.13	0.53	0.92	0.56	0.16	0.96
	stearoylcarnitine	0.46	0.24	0.81	1.14	0.62	0.32	0.87
	oleoylcarnitine	0.44	0.09	0.57	0.87	0.72	0.15	1.08
Carnitine Metabolism	deoxycarnitine	1.18	0.67	0.98	1.02	0.95	0.54	0.98
	carnitine	1.13	0.85	1.05	0.9	1.03	0.78	0.88
	3-dehydrocarnitine	0.84	0.32	0.81	1.2	0.87	0.33	1.29
Ketone Bodies	3-hydroxybutyrate (BHBA)	0.37	0.07	0.79	0.62	0.75	0.15	0.59
Fatty Acid, Monohydroxy	4-hydroxybutyrate (GHB)	0.83	0.46	0.78	0.93	0.55	0.31	0.66
	2-hydroxypalmitate	1.08	0.19	0.8	0.81	0.94	0.16	0.95
	2-hydroxystearate	0.81	0.22	0.77	0.77	0.91	0.25	0.91
	3-hydroxypropanoate	1.3	0.84	0.94	0.87	0.88	0.57	0.81
	3-hydroxydecanoate	0.82	0.28	1.17	0.54	0.92	0.32	0.43
	3-hydroxylaurate	0.61	0.22	1.34	0.61	1.01	0.36	0.46
	16-hydroxypalmitate	0.67	0.17	0.89	0.73	0.95	0.25	0.78
	13-HODE + 9-HODE	1.17	0.14	0.69	0.68	1.19	0.14	1.18
Fatty Acid, Dihydroxy	12,13-DiHOME	1.35	0.24	0.89	0.68	1.06	0.19	0.81
Eicosanoid	12-HETE	1.35	0.15	1.29	1.18	1.52	0.17	1.39
Endocannabinoid	palmitoyl ethanolamide	0.97	0.33	0.86	0.88	1.04	0.35	1.06
Inositol Metabolism	myo-inositol	0.82	0.24	0.62	1.46	0.65	0.19	1.52
	pinitol	1.11	0.94	0.23	20.97	0.37	0.31	33.8
	scyllo-inositol	0.74	0.22	0.57	1.52	0.64	0.19	1.73
	inositol 1-phosphate (IIP)	0.81	0.4	0.95	1.02	0.94	0.47	1.01
Phospholipid Metabolism	choline	0.89	0.4	0.88	1.04	0.89	0.4	1.04
	ethanolamine	1.11	0.59	0.69	1.83	1.12	0.6	2.97
	phosphoethanolamine	1.39	0.74	0.48	1	0.79	0.42	1.64
Lysolipid	2-myristoylglycerophosphocholine*	0.29	0.17	0.81	0.79	0.75	0.45	0.73
	1-pentadecanoylglycerophosphocholine (15:0)*	0.63	0.37	0.9	0.84	0.96	0.57	0.9

1-palmitoylglycerophosphocholine (16:0)	0.69	0.36	0.94	0.97	0.84	0.44	0.86
2-palmitoylglycerophosphocholine*	0.57	0.22	1.01	0.89	0.91	0.34	0.8
1-palmitoleoylglycerophosphocholine (16:1)*	0.24	0.26	0.9	0.79	0.82	0.91	0.72
2-palmitoleoylglycerophosphocholine*	0.35	0.34	0.91	0.93	0.94	0.9	0.96
1-margaroylglycerophosphocholine (17:0)	0.52	0.13	1	0.81	1.03	0.26	0.83
1-stearoylglycerophosphocholine (18:0)	0.61	0.2	0.87	1.01	0.82	0.27	0.95
2-stearoylglycerophosphocholine*	0.67	0.19	1.03	1.25	0.89	0.26	1.08
1-oleoylglycerophosphocholine (18:1)	0.6	0.24	1.04	1.11	0.86	0.35	0.92
2-oleoylglycerophosphocholine*	0.55	0.44	1.07	1.11	0.79	0.64	0.83
1-linoleoylglycerophosphocholine (18:2n6)	0.78	0.38	1.12	1.02	0.88	0.43	0.8
2-linoleoylglycerophosphocholine*	0.53	0.51	1.1	1.13	0.73	0.7	0.75
1-dihomo-linoleoylglycerophosphocholine (20:2n6)*	0.6	0.21	1.41	1.13	0.96	0.33	0.77
2-arachidoylglycerophosphocholine*	0.48	0.23	0.91	0.61	0.94	0.44	0.63
1-eicosatrienoylglycerophosphocholine (20:3)*	0.61	0.41	1.34	1.4	0.75	0.5	0.79
1-arachidonoylglycerophosphocholine (20:4n6)*	0.51	0.23	1.01	1.26	0.79	0.35	0.98
2-arachidonoylglycerophosphocholine*	0.35	0.27	0.83	1.81	0.58	0.45	1.27
1-docosapentaenoylglycerophosphocholine (22:5n3)*	0.93	0.34	1.6	2.7	0.65	0.24	1.09
1-docosahexaenoylglycerophosphocholine (22:6n3)*	0.52	0.25	1.12	1.56	0.71	0.34	0.99
2-docosahexaenoylglycerophosphocholine*	0.54	0.3	1	2.11	0.66	0.36	1.39
1-palmitoylglycerophosphoethanolamine	0.71	0.16	0.95	1.02	0.86	0.19	0.92
2-palmitoylglycerophosphoethanolamine*	0.77	0.47	0.93	1.15	0.78	0.47	0.96
1-stearoylglycerophosphoethanolamine	0.69	0.25	1.2	1.2	0.73	0.27	0.73
1-oleoylglycerophosphoethanolamine	0.81	0.17	0.93	0.85	0.98	0.2	0.9
2-oleoylglycerophosphoethanolamine*	1.09	0.19	1.33	0.85	1.17	0.21	0.75
1-linoleoylglycerophosphoethanolamine*	1.05	0.3	1.01	1.1	0.75	0.21	0.82
2-linoleoylglycerophosphoethanolamine*	0.96	0.36	1	0.96	0.92	0.34	0.88
1-arachidonoylglycerophosphoethanolamine*	0.78	0.23	1.04	1.43	0.75	0.23	1.03
2-arachidonoylglycerophosphoethanolamine*	0.75	0.3	1.29	1.52	0.71	0.28	0.84

		2-docosaehaenoylglycerophosphoethanolamine*	0.36	0.35	0.85	1.11	0.68	0.66	0.89
		1-palmitoylglycerophosphoinositol*	1.28	0.27	1.26	0.96	1.15	0.24	0.87
		1-stearoylglycerophosphoinositol	1.08	0.24	1.09	1.37	0.95	0.21	1.2
		1-linoleoylglycerophosphoinositol*	1.2	0.2	1.54	1.72	1.04	0.17	1.16
		1-arachidonoylglycerophosphoinositol*	1	0.11	1.35	2.43	0.96	0.11	1.73
		2-arachidonoylglycerophosphoinositol*	0.84	0.1	1.34	1.95	1.15	0.14	1.68
	Glycerolipid Metabolism	glycerol	0.93	0.62	0.82	0.78	1	0.67	0.95
	Glycerolipid Metabolism	glycerol 3-phosphate (G3P)	0.89	0.21	0.74	1.15	0.94	0.22	1.46
	Monoacylglycerol	1-palmitoylglycerol (1-monopalmitin)	0.91	0.22	0.64	1.5	0.74	0.18	1.75
	Monoacylglycerol	1-stearoylglycerol (1-monostearin)	1.21	0.36	1.42	1.21	0.81	0.24	0.69
	Monoacylglycerol	1-oleoylglycerol (1-monoolein)	1.58	0.37	0.67	1.38	0.63	0.15	1.29
	Monoacylglycerol	1-linoleoylglycerol (1-monolinolein)	1.81	0.26	0.73	1.18	0.8	0.11	1.31
	Sphingolipid Metabolism	sphinganine	0.4	0.27	0.72	0.79	0.56	0.37	0.61
	Sphingolipid Metabolism	palmitoyl sphingomyelin	0.65	0.19	0.75	1.24	0.73	0.21	1.2
	Sphingolipid Metabolism	stearoyl sphingomyelin	0.78	0.12	0.69	1.08	0.66	0.1	1.03
	Sphingolipid Metabolism	sphingosine	0.9	0.23	0.74	0.49	1.66	0.42	1.1
	Sterol	cholesterol	0.84	0.37	0.87	1.43	0.74	0.33	1.21
	Sterol	7-alpha-hydroxy-3-oxo-4-cholestenoate (7-Hoca)	0.84	0.23	0.84	1.21	0.89	0.25	1.29
	Sterol	cholestanol	0.66	0.47	0.72	1.5	0.66	0.47	1.38
	Sterol	beta-sitosterol	0.82	0.66	1.14	1.7	0.63	0.51	0.95
	Sterol	campesterol	0.75	0.41	0.86	1.24	0.7	0.39	1.02
	Steroid	corticosterone	0.7	0.14	0.75	1.03	0.88	0.17	1.21
	Primary Bile Acid Metabolism	cholate	1.02	0.5	0.32	5.22	0.2	0.1	3.28
	Primary Bile Acid Metabolism	glycocholate	0.64	0.85	0.13	4.25	0.14	0.19	4.8
	Primary Bile Acid Metabolism	taurocholate	0.43	0.07	0.01	12.19	0.05	0.01	40.9
	Primary Bile Acid Metabolism	beta-muricholate	2.18	0.27	1.26	1.18	0.92	0.11	0.86
	Primary Bile Acid Metabolism	alpha-muricholate	0.14	0.34	0.01	25.44	0.03	0.08	62.35
	Secondary Bile Acid Metabolism	deoxycholate	0.9	0.2	1.09	0.97	1.44	0.33	1.29
	Secondary Bile Acid Metabolism	taurodeoxycholate	0.3	0.17	0.03	14.26	0.04	0.02	23.63
	Secondary Bile Acid Metabolism	tauroolithocholate	0.47	1	0.05	26.96	0.05	0.11	26.96
	Secondary Bile Acid Metabolism	tauroursodeoxycholate	0.51	0.08	0.01	32.09	0.04	0.01	94.96
Nucleotide	Purine Metabolism, (Hypo)Xanthine/Inosi	inosine	0.93	0.13	1.35	0.48	0.5	0.07	0.18
	Purine Metabolism, (Hypo)Xanthine/Inosi	hypoxanthine	1.58	0.04	0.96	2.22	1.59	0.04	3.66

	ne containing	xanthine	1.74	0.05	0.93	1.3	2.03	0.06	2.84
		xanthosine	2.24	0.4	0.68	1.63	1.09	0.19	2.63
		urate	1.35	0.12	0.7	0.93	1	0.09	1.32
		allantoin	0.47	0.18	0.38	4.25	0.46	0.18	5.16
	Purine Metabolism, Adenine containing	adenosine 5'-monophosphate (AMP)	0.94	34.51	0.72	1.36	0.72	26.41	1.36
		adenine	0.67	0.58	0.67	4.69	0.54	0.47	3.77
		N1-methyladenosine	0.6	0.31	0.46	3.55	0.56	0.28	4.28
		N6-carbamoylthreonyladenosine	0.56	0.33	0.5	4.66	0.55	0.33	5.07
	Purine Metabolism, Guanine containing	7-methylguanine	0.77	1.11	0.35	3.81	0.57	0.82	6.21
		N1-methylguanosine	0.62	0.73	0.37	4.56	0.5	0.59	6.19
	Pyrimidine Metabolism, Orotate containing	orotate	0.56	0.58	0.56	4.55	0.48	0.5	3.93
	Pyrimidine Metabolism, Uracil containing	uridine	1.34	0.56	1.06	0.75	0.96	0.41	0.69
		uracil	2	0.53	0.78	0.89	1.07	0.28	1.23
		pseudouridine	0.92	0.68	0.84	2.45	0.68	0.5	2.01
		5,6-dihydrouracil	0.79	0.38	1.08	1.23	1.18	0.56	1.33
		2'-deoxyuridine	1.04	0.53	0.97	1.18	0.72	0.37	0.88
		3-ureidopropionate	0.7	0.17	0.38	2.37	0.55	0.14	3.43
		N-acetyl-beta-alanine	1.17	0.51	0.86	1.71	0.8	0.35	1.6
	Pyrimidine Metabolism, Cytidine containing	cytidine	1.12	0.38	0.85	0.73	0.95	0.32	0.82
		N4-acetylcytidine	0.79	0.76	0.75	1.97	0.85	0.82	2.23
2'-deoxycytidine		0.85	0.58	0.88	1.08	0.75	0.52	0.92	
Pyrimidine Metabolism, Thymine containing	thymidine	0.8	0.47	0.93	0.79	0.76	0.45	0.64	
Cofactors and Vitamins	Nicotinate and Nicotinamide Metabolism	nicotinamide	0.94	0.2	0.68	1.02	0.95	0.2	1.42
	Riboflavin Metabolism	riboflavin (Vitamin B2)	0.75	0.4	0.42	5.04	0.45	0.24	5.39
		flavin adenine dinucleotide (FAD)	1.05	0.65	0.99	1	0.9	0.56	0.91
	Pantothenate and CoA Metabolism	pantothenate	1.08	0.25	0.81	2.24	0.75	0.17	2.06
	Ascorbate and Aldarate Metabolism	gulono-1,4-lactone	0.44	0.19	0.32	6.03	0.3	0.13	5.73
		ascorbate (Vitamin C)	0.98	0.27	0.48	4.39	0.32	0.09	2.9
		threonate	0.79	0.08	0.66	1.69	0.76	0.08	1.94
arabonate		0.47	0.17	0.32	3.89	0.51	0.18	6.21	

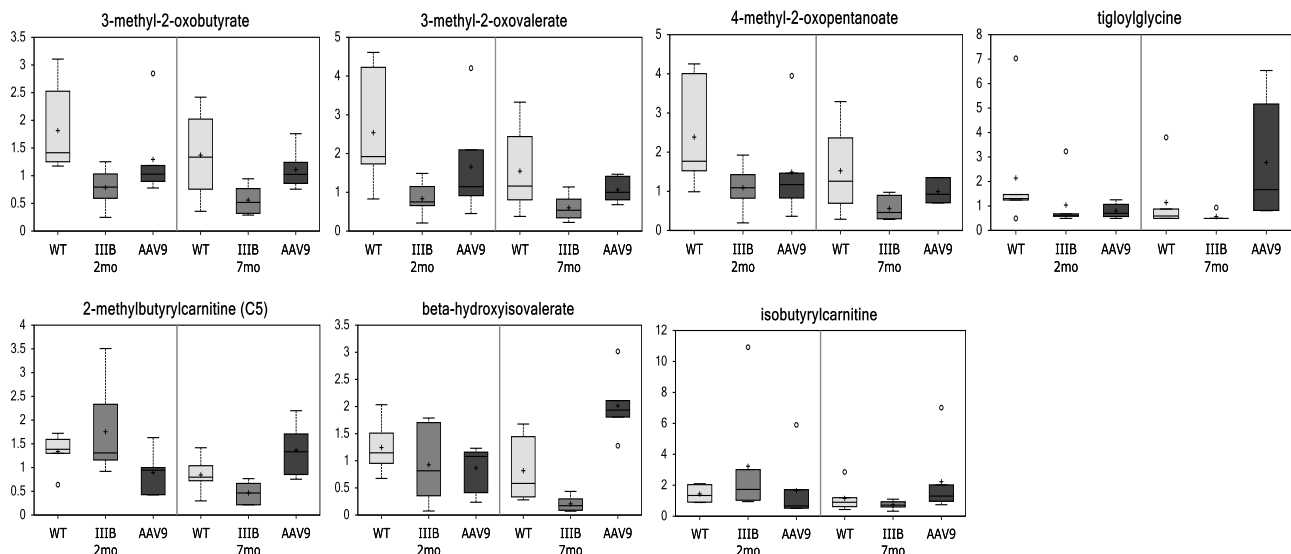
		oxalate (ethanedioate)	0.7	0.43	0.79	1.48	0.68	0.42	1.28
	Tocopherol Metabolism	alpha-tocopherol	0.85	0.18	1.05	1.29	0.84	0.18	1.03
	Tetrahydrobiopterin Metabolism	dihydrobiopterin	0.53	0.23	0.35	4.13	0.43	0.19	5.07
	Hemoglobin and Porphyrin Metabolism	heme	0.95	1.09	1.31	0.67	1.04	1.2	0.53
		bilirubin (E,E)*	0.38	0.5	0.67	0.65	1.12	1.49	1.09
		biliverdin	0.81	0.31	1.03	0.88	0.95	0.36	0.81
		L-urobilin	1	1	1	1	1	1	1
	Vitamin B6 Metabolism	pyridoxate	0.63	0.24	0.38	6.33	0.45	0.17	7.57
Xenobiotics	Benzoate Metabolism	hippurate	0.36	0.4	0.28	9.78	0.48	0.53	16.34
		4-hydroxyhippurate	0.28	0.26	0.15	3.39	0.56	0.52	12.9
		benzoate	0.8	0.84	1.24	1.33	1.13	1.17	1.21
		catechol sulfate	0.72	0.46	0.43	5.15	0.73	0.47	8.72
		4-ethylphenylsulfate	0.8	0.61	0.49	7.1	0.49	0.37	7.08
		4-vinylphenol sulfate	0.49	0.06	0.61	1.15	0.72	0.09	1.35
	Food Component/Plant	2-oxindole-3-acetate	0.64	0.6	0.43	13.25	0.41	0.38	12.72
		5-hydroxymethylfurfural	0.9	0.36	0.94	0.97	0.77	0.31	0.8
		cinnamoylglycine	0.22	0.22	0.26	5.1	0.59	0.6	11.51
		daidzein	0.9	1	0.9	4.56	0.9	1	4.56
		equol glucuronide	0.82	0.61	0.36	33.73	0.22	0.16	20.59
		equol sulfate	1.17	0.82	0.95	4.59	0.68	0.48	3.3
		ergothioneine	0.67	0.36	0.7	1.37	1.26	0.67	2.46
		erythritol	0.61	0.34	0.39	4.33	0.55	0.31	6.13
		galacturonate	0.65	0.4	0.67	3.94	0.71	0.43	4.18
		indoleacrylate	1.57	0.93	1.33	1.63	0.7	0.42	0.87
		N-(2-furoyl)glycine	0.21	0.42	0.22	4.5	0.5	1	10.38
		N-glycolylneuramate	0.64	0.07	0.15	0.81	0.59	0.06	3.1
		stachydrine	1.53	0.73	1.09	2.31	0.79	0.38	1.68
	Drug	4-acetylphenol sulfate	0.26	0.55	0.24	15.54	0.37	0.8	24.54
	Chemical	1-(3-aminopropyl)-2-pyrrolidone	0.42	0.54	0.39	3.84	0.42	0.54	4.09
		2-ethylhexanoate	0.67	0.34	0.91	1.39	1.09	0.54	1.67
		2-hydroxyisobutyrate	0.76	0.51	1.08	1.31	0.89	0.6	1.07
diisopropanolamine		0.56	0.38	0.85	0.77	1.1	0.74	0.99	
EDTA		1	1.13	1	1	1	1.13	1	

	glycolate (hydroxyacetate)	0.83	0.36	0.73	1.39	0.71	0.31	1.35
	iminodiacetate (IDA)	1	1.49	1	1	1	1.49	1
	trizma acetate	0.76	84.69	0.61	3.98	1.05	117.21	6.82

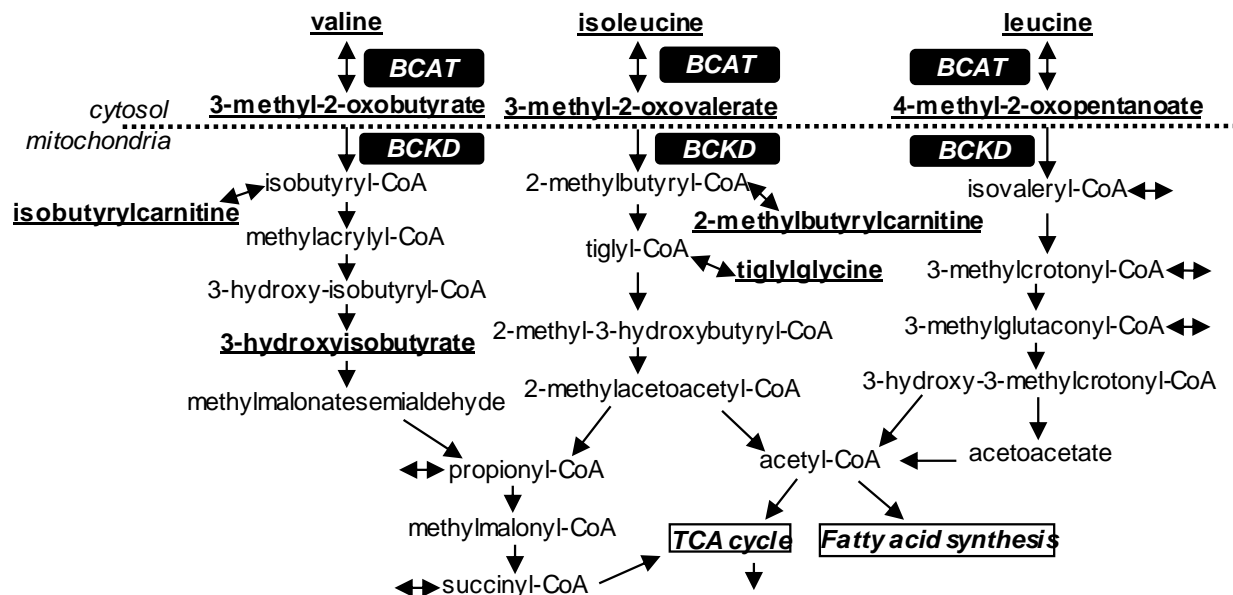
Serum samples were assayed for 361 metabolites at 2mo and 7mo of age, using mass spectrometry (n=6/group).

Green highlight: decrease, $p \leq 0.05$; Light green highlight: decrease, $0.05 < p < 0.10$; Red highlight: increase, $p \leq 0.05$; Pink highlight: increase, $0.05 < p \leq 0.10$; No highlight: $p > 0.10$.

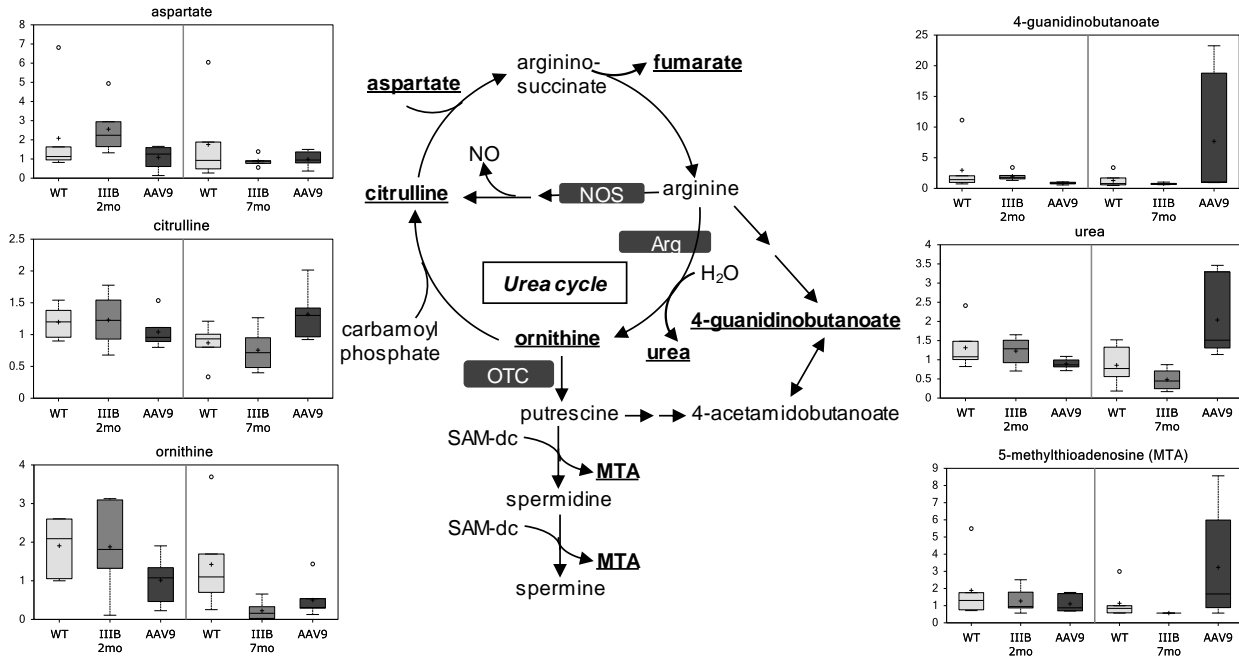
a.



b.

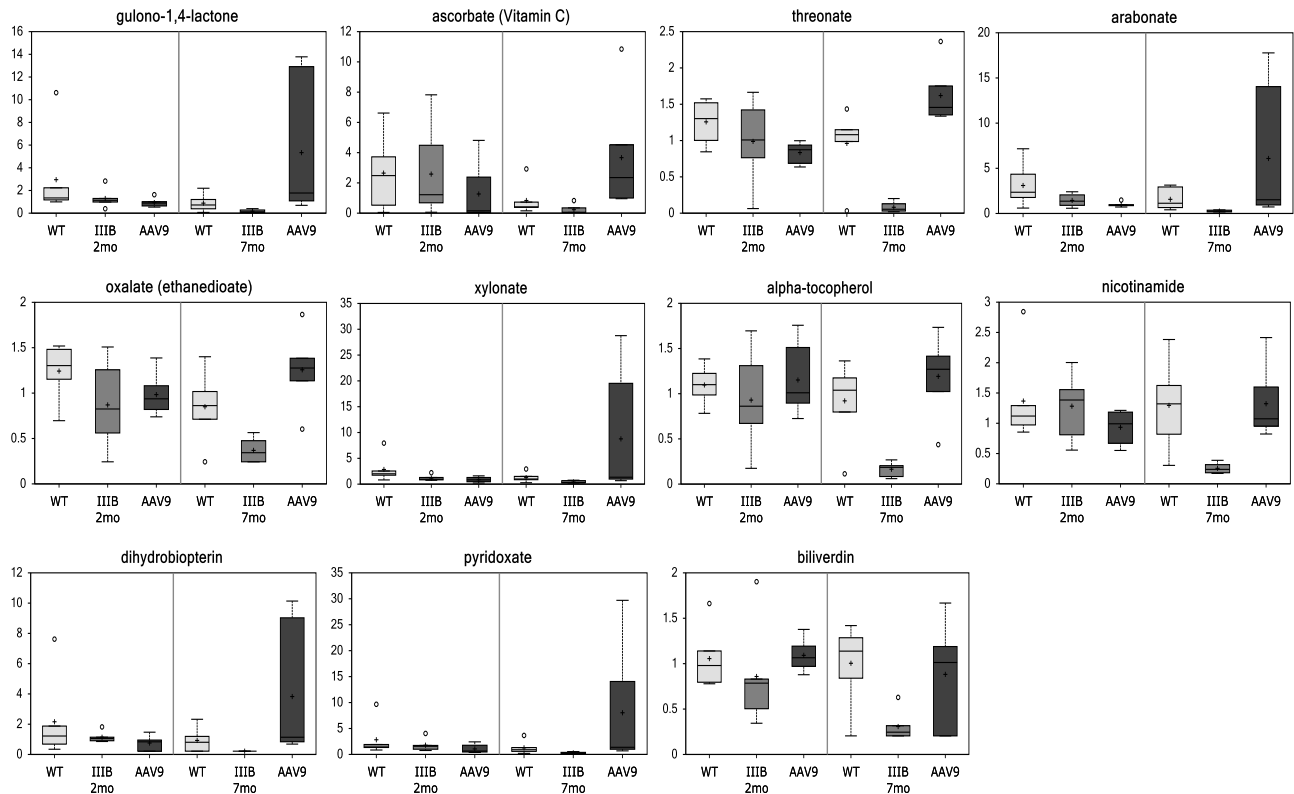


Supplementary Fig. S1 Impairments of branched-chain amino acid metabolism during disease progression in MPS IIIB mice Mouse serum samples were analyzed by global metabolomic profiling using mass spectrometry at age 2m or 7mo (n=6/group). **a.** Metabolomic comparison: data are presented as Scaled Intensity (y-axis), $p \leq 0.05$ IIIB-7m vs. WT-7m; **WT**: wildtype mice; **IIIB**: MPS IIIB mice; **AAV9**: MPS IIIB mice treated at age 1m with an IV injection of 5×10^{12} vg/kg rAAV9-CMV-hNAGLU. **b.** Branched-chain amino acid metabolism pathway: **BCAT**: branched chain aminotransferase; **BCKD**: branched-chain alpha-keto acid dehydrogenase complex; Bold and underlined metabolites: $p \leq 0.05$ IIIB-7m vs. WT-7m.

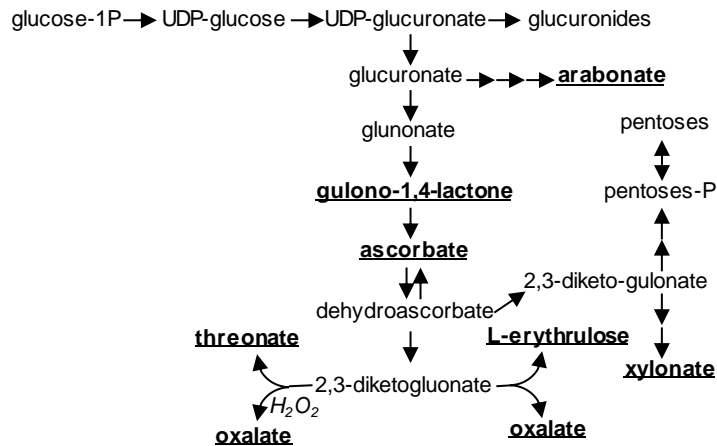


Supplementary Fig. S2. Impairments of urea cycle during disease progression in MPS III B mice Mouse serum samples were analyzed by global metabolomic profiling using mass spectrometry at age 2mo or 7mo (n=6/group). **a.** Metabolomic comparison: data are presented as Scaled Intensity (y-axis), $p \leq 0.05$ IIB-7m vs. WT-7m; **WT**: wildtype mice; **IIB**: MPS III B mice; **AAV9**: MPS III B mice treated at age 1m with an IV injection of 5×10^{12} vg/kg rAAV9-CMV-hNAGLU. Bold and underlined metabolites in urea cycle pathway: $p \leq 0.05$ IIB-7m vs. WT-7m.

a.

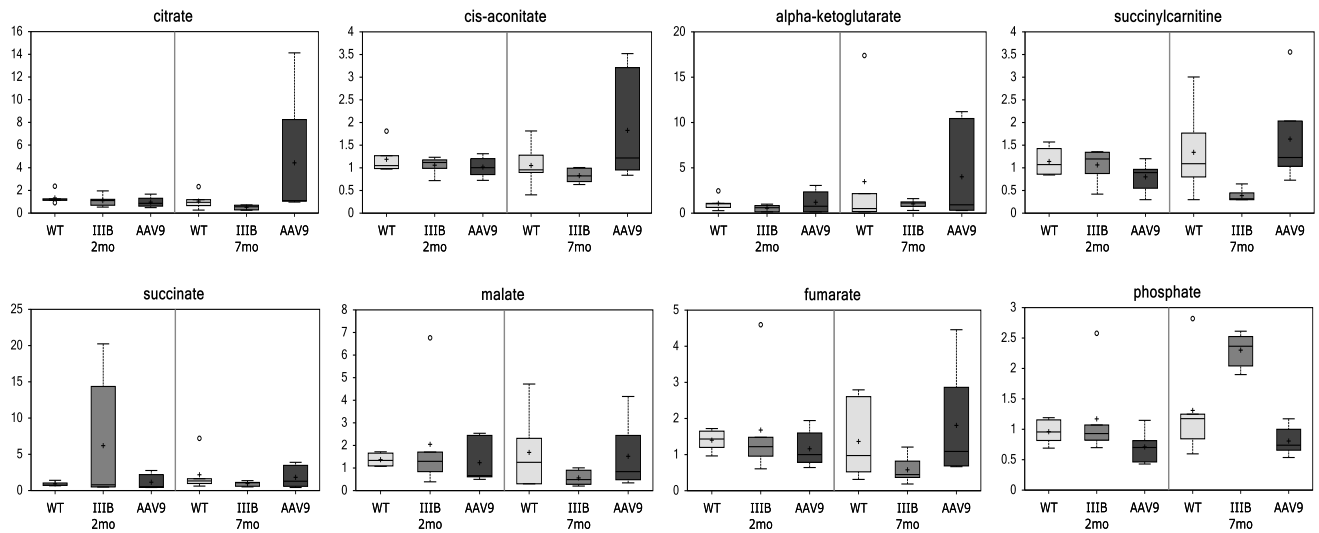


b. Ascorbate (Vitamin C) metabolism pathway

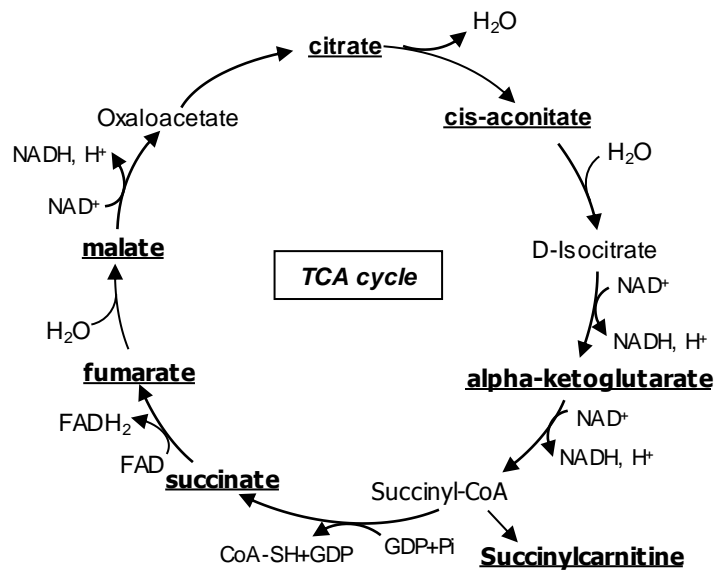


Supplementary Fig. S3. Depressed Vitamin metabolism in MPS IIB during disease progress Mouse serum samples were analyzed by global metabolomic profiling using mass spectrometry at age 2m or 7mo (n=6/group). **a.** Metabolomic comparison: data are presented as Scaled Intensity (y-axis), $p \leq 0.05$ IIB-7m vs. WT-7m; **WT**: wildtype mice; **IIB**: MPS IIB mice; **AAV9**: MPS IIB mice treated at age 1m with an IV injection of 5×10^{12} vg/kg rAAV9-CMV-hNAGLU. **b.** Disturbance of Vitamin C metabolism pathway: Bold and underlined metabolites: $p \leq 0.05$ IIB-7m vs. WT-7m.

a.



b. TCA pathway



Supplementary Fig. S4. Depressed energy metabolism in MPS IIB during disease progress Mouse serum samples were analyzed by global metabolomic profiling using mass spectrometry at age 2m or 7mo ($n=6$ /group). **a.** Metabolomic comparison: data are presented as Scaled Intensity (y-axis), $p \leq 0.05$ IIB-7m vs. WT-7m; **WT**: wildtype mice; **IIB**: MPS IIB mice; **AAV9**: MPS IIB mice treated at age 1m with an IV injection of 5×10^{12} vg/kg rAAV9-CMV-hNAGLU. **b.** Disturbance of energy metabolism pathway: Bold and underlined metabolites: $p \leq 0.05$ IIB-7m vs. WT-7m.